# CHAPTER IV

RESULTS AND DISCUSSION

The aim of this work was to modify DBS molecule for using as a nucleating agent and study their effect on mechanical properties and morphology of polypropylene fiber. Sorbitol derivatives were prepared by acid catalysis reaction of D-sorbitol with an aromatic aldehyde in cyclohexane. Sorbitol derivatives were characterized by FTIR and NMR spectroscopy. The iPP containing sorbitol derivatives were prepared by using solution blending and melt blending process using two-roll mill. Mechanical properties of neat iPP and iPP fiber containing sorbitol derivatives were investigated by using tensile tester. Morphology of neat iPP and iPP fiber containing sorbitol derivatives were investigated by using SEM technique.

In this chapter, the results are composed of six sections. The first section is the synthesis and characterization of sorbitol derivatives, respectively. The second section is gel formation and fibril morphology. The third section is the effect of sorbitol derivatives on crystallization, melting temperature and degree of crystallinity nucleation and crystallization of iPP. The fourth section is the effect of sorbitol derivatives on the morphology and orientation of iPP fiber. The fifth section is the effect of sorbitol derivatives on mechanical properties of iPP fiber, respectively. The details of each section are shown below.

Synthesis of sorbitol derivatives and characterization of sorbitol derivatives

In this work, sorbitol derivatives were synthesized for using as a nucleating agent of iPP. The sorbitol derivatives were prepared by reacting 2 moles of halogenated aromatic aldehyde (such as chloro and bromo-benzaldehyde) with 1 mole of D-sorbitol in cyclohexane. As a reaction in the presence of an acid catalyst occur at an elevated temperature thereby to perform dehydrocondensation. For chloro derivatives, different positions of substitution which including *ortho*, *meta* and *para*

were also synthesized. The procedure for various sorbitol derivatives syntheses were shown in Figure 24.
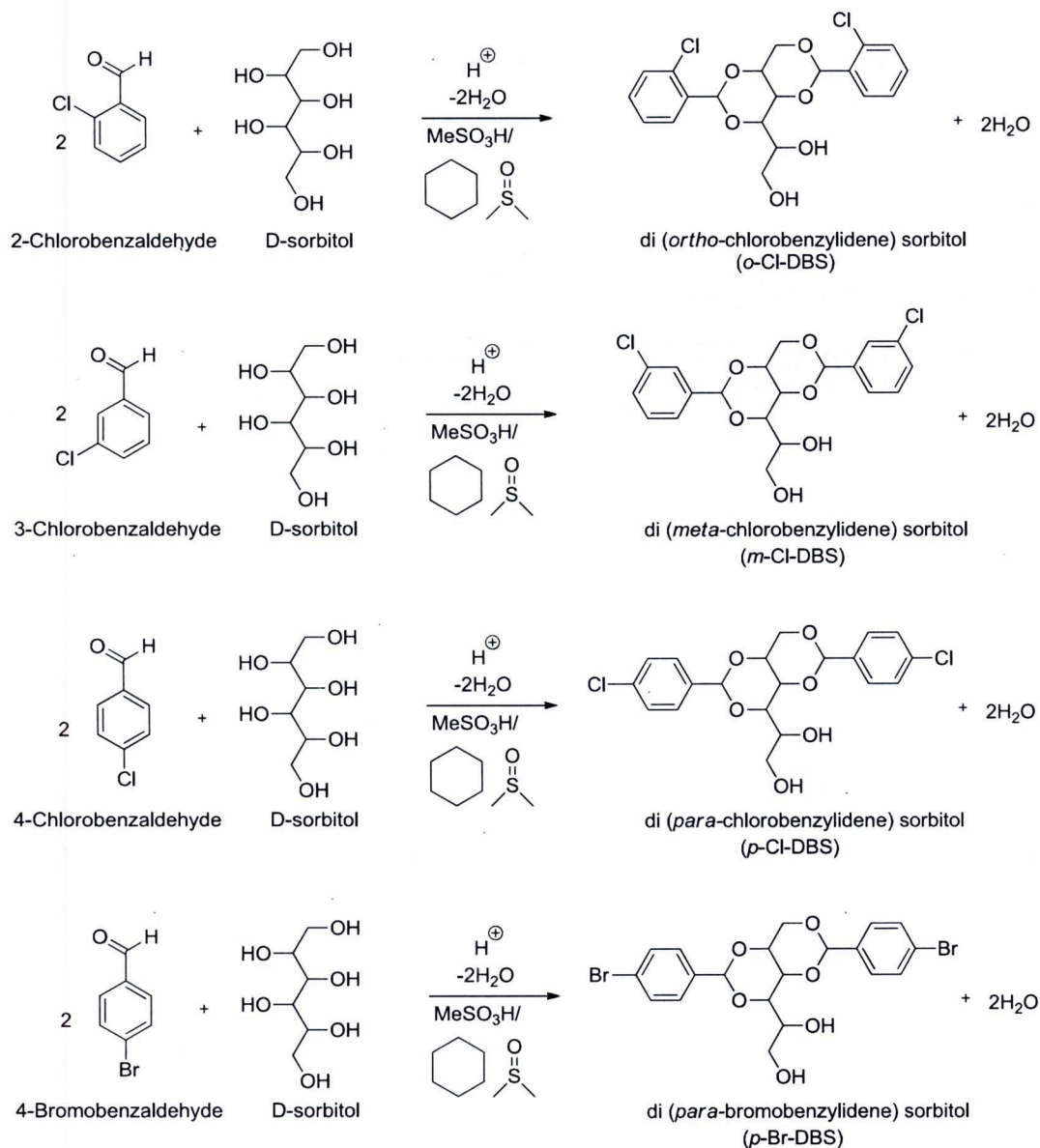
Figure 24 Synthesis of various sorbitol derivatives

It was found that the percentage yield of *p*-Cl-DBS and *p*-Br-DBS are higher than *o*-Cl-DBS and *m*-Cl-DBS as shown in Table 4. Since chloro derivative in *para* position is far from carbonyl group of aldehyde, so the reaction is easy to occur. When two positions of 1,3:2,4- and 1,3:4,5- are compared, it was found that the reaction on 1,3:2,4- position can react better than the other. This is due to the benzylic ring which is in the 4,5- position is a fifth memberd ring and not flexible. Therefore, the reaction in this position is quite difficult to occur. The percentage yield of *p*-Cl-DBS is similar to *p*-Br-DBS.

Table 4 The percentage of yield of sorbitol derivatives

Sample	% yield
1,3:2,4-di(2-chlorobenzylidene) sorbitol (*o*-Cl-DBS)	36
1,3:2,4-di(3-chlorobenzylidene) sorbitol (*m*-Cl-DBS)	36
1,3:2,4-di(4-chlorobenzylidene) sorbitol (*p*-Cl-DBS)	54
1,3:2,4-di(4-bromobenzylidene) sorbitol (*p*-Br-DBS)	50

In this study, the sorbitol derivatives were characterized by using melting apparatus, DSC technique, FTIR spectroscopy and NMR spectroscopy. These techniques employed to confirm the thermal properties and chemical structure of sorbitol derivatives.

Melting temperature of sorbitol derivatives

In this topic the melting temperature was used to confirm the thermal properties of products, which derived from the reaction of D-sorbitol and aromatic benzaldehyde.

The melting temperature of sorbitol derivatives are shown in Table 5. These were obtained from melting apparatus and DSC technique. For melting apparatus, each sample was heated from 50 °C with a heating rate of 2 °C/min until the sample begin melt. Each sample was repeated 3 times. For DSC technique, each sample was heated from 120 °C to 260 °C with heating rate of 10 °C/min. After that they were cooled with a cooling rate of 5 °C/min and then the sample was reheated with a

heating rate of 10 °C/min. The melting point of D-sorbitol is in range 94°C to 98 °C [64]. Table 5 shows that the melting point of D-sorbitol and sorbitol derivatives are different. These results confirm that the produced substances are really sorbitol derivatives. The melting reference of DBS is in range 220 °C to 225 °C [43,44]. It can be seen that the melting point of DBS and derivatives are lower than the melting temperature of the reference. This indicates that the sorbitol derivatives derives from the reaction mixture are not 100 % pure.

Table 5 Melting temperature of sorbitol derivatives by melting apparatus and DSC technique

Sample	Reference (°C)	Melting temperature by DSC (°C)		Melting apparatus (°C)			
		onset	peak	1	2	3	average
DBS	220-225[44]	-	-	230.6-234.7	229.1-235.9	229.0-235.7	229.6-235.4
o-Cl-DBS	220-222[55]	158.32	159.97	136.7-148.5	137.5-145.6	137.4-148.3	137.2-147.5
m-Cl-DBS	-	177.05	181.28	162.0-166.6	162.9-166.0	162.8-170.0	162.6-167.5
p-Cl-DBS	244-247[55]	185.50	192.44	211.7-217.7	211.9-215.0	211.5-215.0	211.7-215.9
p-Br-DBS	-	193.63	194.76	153.5-162.4	155.0-161.2	154.4-162.6	154.3-162.1

Functional group characterization by FT-IR spectroscopy

FT-IR spectroscopy was employed to characterize the functional groups of reactant for example D-sorbitol and 4-chlorobenzalhehyde and sorbitol derivatives. Figure 25 shows FT-IR spectra of reactant (D-sorbitol and 4-chlorobenzaldehyde). For D-sorbitol, the present of an O-H and C-H stretching of alcohol in the signal of 3325 and 1096 cm^{-1} and C-H stretching and C-H blending of alkane in the signal of 2931 cm^{-1} and at 1419 and 377 cm^{-1} can be observed, respectively. While a C-H and C=C stretching of aromatic in the vicinity of 3880 cm^{-1} and at 1588 and 1575 cm^{-1}, C-H and C=O stretching of aldehyde in the signal of 2859 and 1700 cm^{-1}, C-H blending out of plane *para* and C-Cl stretching in the signal of 815 and 707 cm^{-1} can be seen for 4-chrolobenzaldehyde. All assigned functional groups of reactants were shown in Table 6.
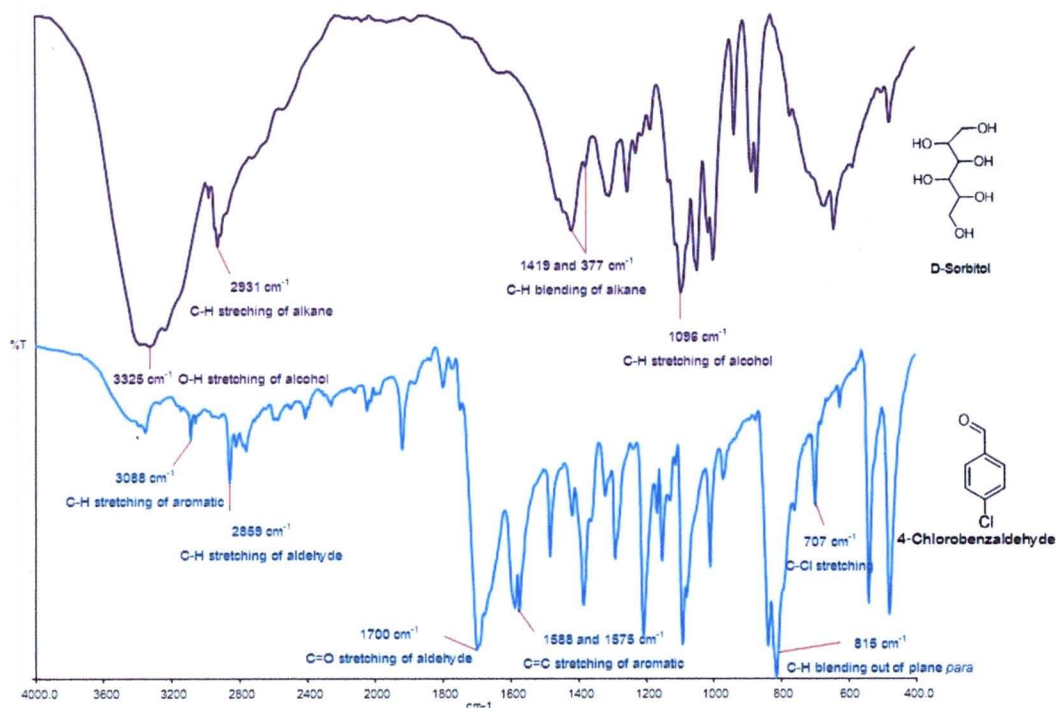
Figure 25 FT-IR spectra of D-sorbitol (upper) and 4-chlorobenzaldehyde (lower)

Table 6 Functional group annotation of D-sorbitol and 4-chlorobenzaldehyde

Sample	Wave number (cm^{-1})	Functional groups
	1047.8	C-O stretching of 1° alcohol
	1096.1	C-O stretching of 2° alcohol
D-sorbitol	1419.0 and 1377.6	C-H blending of alkane
	2943.0	C-H stretching of alkane
	3325.4	O-H stretching of alcohol
	707.0	C-Cl stretching
	815.2	C-Cl blending out of plane of para
4-chlorobenzyldehyde	1588.2 and 1575.0	C=C stretching of aromatic
	1700.7	C=O stretching of aldehyde
	2859.2	C-H stretching of aldehyde
	3088.9	C-H stretching of aromatic
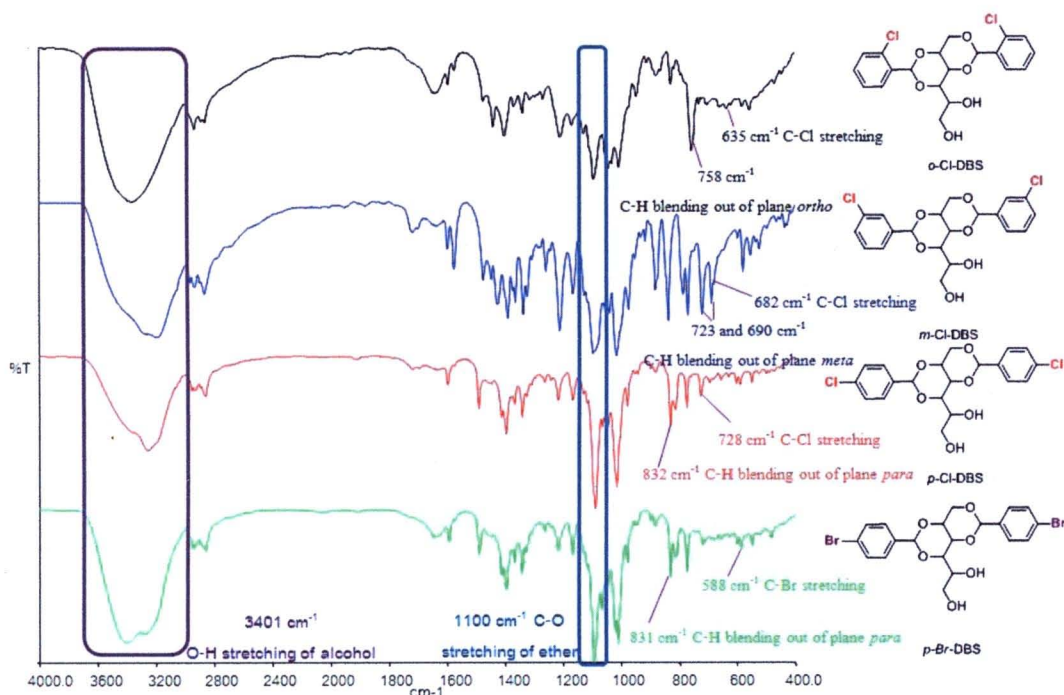
Figure 26 FT-IR spectra of sorbitol derivatives

The sorbitol derivatives were synthesized by reacting D-sorbitol and aromatic benzaldehyde derivative which was substituted in either of the *ortho*, *meta* and *para* position with a halogen atom selected from Cl and Br. Functional groups were characterized by FT-IR spectroscopy. From the FT-IR spectra, the presences of a C-O stretching of ether at 1100 cm^{-1} can be observed for all derivatives. This signal can be only seen in the products not in the reactants. The products were substituted with *ortho*, *meta* and *para* positions for chloro derivatives show signals of C-H blending out of plane at 758, 723 and 690, and 832 cm^{-1}, respectively. The presences of signals at 635, 682 and 728 cm^{-1} were also observed the C-Cl stretching of the three substitutions, respectively. For bromo derivatives, the presence of the signal of C-H blending out of plane at 831 cm^{-1} and signal of C-Br stretching at 588 cm^{-1} can be observed. Therefore, it can be confirmed that the products are from the reaction between D-sorbitol and aromatic benzaldehyde. All assigned functional groups of the derivatives and their wave numbers are shown in Table 7.

Table 7 Functional group annotation of *o*-Cl-DBS, *m*-Cl-DBS, *p*-Cl-DBS and *p*-Br-DBS

Sample	Wave number (cm^{-1})	Functional groups
o-Cl-DBS	635.2	C-Cl stretching
	758.9	C-H bending out of plane of ortho
	1050.5	C-O stretching of 1°alcohol
	1098.1	C-O stretching of ether
	1405.0 and 1324.0	C-H bending of alkane
	1598.3 and 1576.4	C=C stretching of aromatic
	2937.3 and 2891.2	C-H stretching of alkane
	3369.0	O-H stretching of alcohol
m-Cl-DBS	682.0	C-Cl stretching
	723.0 and 690.3	C-H bending out of plane of meta
	1019.2	C-O stretching of 1°alcohol
	1100.8	C-O stretching of ether
	1429.9 and 1394.4	C-H bending of alkane
	1601.5 and 1579.2	C=C stretching of aromatic
	2936.2 and 2871.8	C-H stretching of alkane
	3200.6	O-H stretching of alcohol

51

Table 7 (Cont.)

Sample	Wave number (cm-1)	Functional groups
p-Cl-DBS	728.1	C-Cl stretching
	832.4	C-H bending out of plane of para
	1016.7	C-O stretching of 1°alcohol
	1090.8	C-O stretching of ether
	1416.4 and 1399.1	C-H bending of alkane
	1601.1 and 1494.6	C=C stretching of aromatic
	2942.6 and 2866.4	C-H stretching of alkane
	3263.8	O-H stretching of alcohol
p-Br-DBS	588.0	C-Br stretching
	831.0	C-H bending out of plane of para
	1021.9	C-O stretching of 1°alcohol
	1169.0	C-O stretching of ether
	1414.3 and 1399.6	C-H bending of alkane
	1595.5 and 1490.9	C=C stretching of aromatic
	2942.2 and 2864.6	C-H stretching of alkane
	3401.2	O-H stretching of alcohol

Chemical structure characterization by NMR

NMR spectroscopy was used to interpret and confirm the chemical structure of sorbitol derivatives. The ^{1}H NMR spectra of reactants for example D-sorbitol and 4-chlorobezaldehyde are shown in Figure 27.
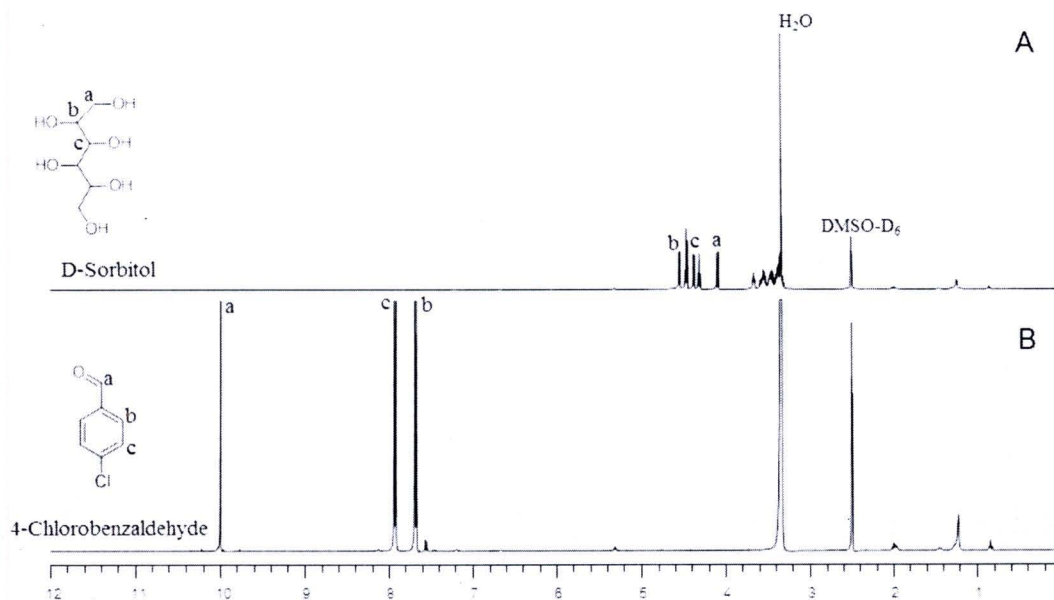
Figure 27 ^{1}H NMR spectra of A) D-sorbitol and B) 4-chlorobenzaldehyde (use DMSO-D$_6$ as a solvent)

The spectrum A reveals the presence of signal b (4.55ppm), signal c (4.38 ppm) and signal a (3.45 ppm) which are corresponding to alkane protons for D-sorbitol. For 4-chlorobezaldehyde, the signal at 10 ppm corresponds to aldehyde protons and the signal c and b (7.92 and 7.69 ppm) corresponding to aromatic protons. All assigned functional groups of both reactants were listed in detail in Table 8.

Table 8 Chemical shift of reactants (use DMSO-D$_6$ as a solvent)

Sample	Chemical shift (ppm)	area	position	proton
	4.55	1.0	b	H-alkane
D-sorbitol	4.38	0.9	c	H-alkane
	3.45	2.2	a	H-alkane
	10.00	1.0	a	H-aldehyde
4-chlorobenzaldehyde	7.92	2.2	c	H-aromatic
	7.69	2.0	b	H-aromatic

The chemical structure of sorbitol derivatives were confirmed by ^{1}H NMR spectroscopy (Figure 28 and Table 9). It can be seen that the signal at 10 ppm which corresponds to aldehyde protons were disappeared for all derivatives. Meanwhile the signal a (about 5.6-5.7 ppm) can be cleary seen. This indicates the present of benzylic protons.
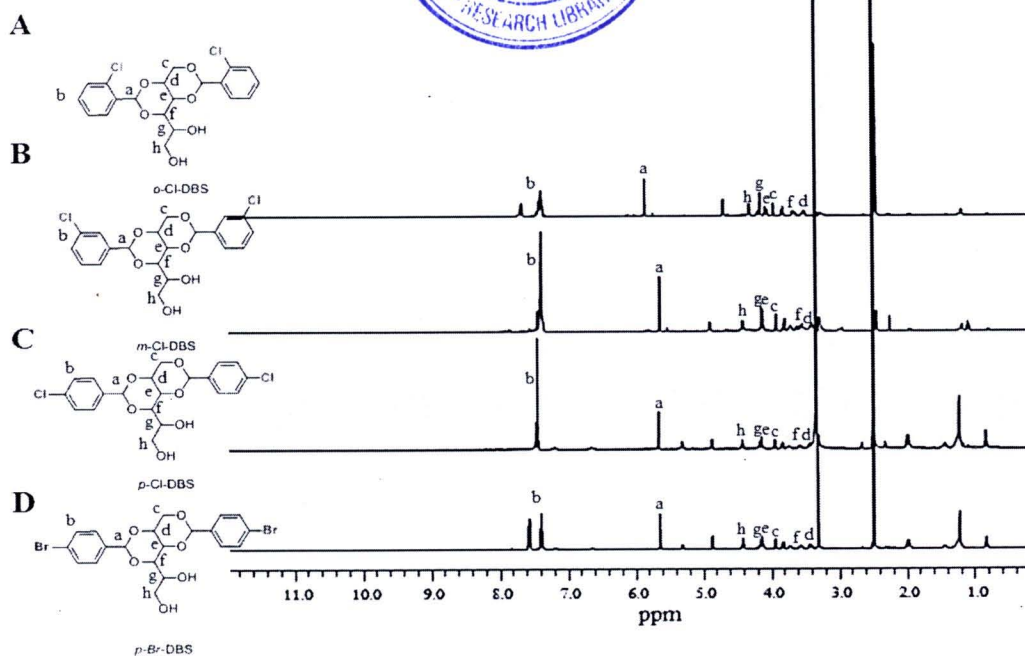
Figure 28 ^{1}H NMR spectra of sorbitol derivatives

These materials were substituted with *ortho, meta* and *para* positions for chloro derivatives. It was found that the signal of benzylic protons (signal a) of *ortho* position (*o*-Cl-DBS) was higher than that of *meta* (*m*-Cl-DBS) and *para* (*p*-Cl-DBS) position. Due to the chlorine atom on the *ortho* position is closed to the benzylic protons, so the electron cloud of chlorine atom can hide the proton at the benzylic position of this position more than the other positions. As a result the chemical shift of *ortho* position is higher than the other derivatives.

Table 9 Chemical shift of sorbitol derivatives (use DMSO-D$_6$ as a solvent)

Sample	Chemical shift (ppm)	area	position	proton
o-Cl-DBS	7.44	8.1	b	H-aromatic
	5.90	0.9	a	H-benzylic
	4.34	1.8	h	H-alkane
	4.20	1.2	g	H-alkane
	4.10	1.0	e	H-alkane
	4.00	1.8	c	H-alkane
	3.86	1.2	f	H-alkane
	3.61	0.9	d	H-alkane
m-Cl-DBS	7.42	8.3	b	H-aromatic
	5.69	1.0	a	H-benzylic
	4.47	1.8	h	H-alkane
	4.19	1.3	g	H-alkane
	4.16	1.3	e	H-alkane
	3.84	2.3	c	H-alkane
	3.62	1.0	f	H-alkane
	3.47	1.4	d	H-alkane
p-Cl-DBS	7.45	8.4	b	H-aromatic
	5.67	1.0	a	H-benzylic
	4.45	1.7	h	H-alkane
	4.18	1.0	g	H-alkane
	4.14	1.2	e	H-alkane
	3.95	1.8	c	H-alkane
	3.67	1.1	f	H-alkane
	3.56	1.0	d	H-alkane

Table 9 (Cont.)

Sample	Chemical shift (ppm)	area	position	proton
	7.55	7.8	b	H-aromatic
	5.66	1.0	a	H-benzylic
	4.44	1.6	h	H-alkane
p-Br-DBS	4.18	1.4	g	H-alkane
	4.15	1.0	e	H-alkane
	3.95	1.8	c	H-alkane
	3.60	1.2	f	H-alkane
	3.45	1.3	d	H-alkane

The ^{13}C NMR spectroscopy is analogous to ^{1}H NMR and allows the identification of carbon atoms in organic molecule just as ^{1}H NMR identifies hydrogen atoms.

Figure 29 shows ^{13}C NMR spectrum to confirm the formation of *p*-Cl-DBS. It shows signal a (138.90 ppm), signal b (133.45 ppm), signal c (128.53 ppm), signal d (98.53 ppm), signal e (77.89 ppm), signal f (70.46 ppm), signal g (69.66 ppm), signal h (68.81 ppm), signal i (67.95 ppm), and signal j (62.92 ppm) corresponding to CC, CCl, CH, CO, CH, CH, CH_2, CH, CH, and CH_2 carbons for *p*-Cl-DBS.
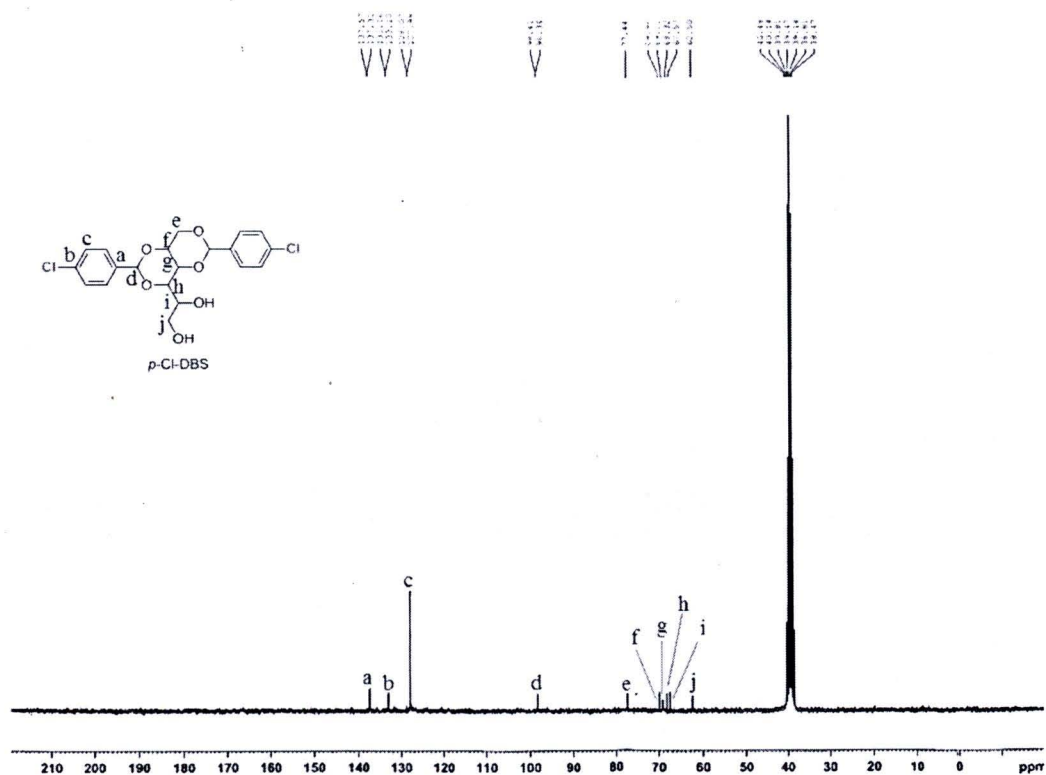
Figure 29 ^{13}**C NMR spectrum of** *p*-**Cl-DBS**

Table 10 Chemical shift of *p*-Cl-DBS

Chemical shift (ppm)	Position	Carbon
62.92	j	CH$_2$
67.95	i	CH
68.81	h	CH
69.66	g	CH$_2$
70.46	f	CH
77.89	e	CH
98.53	d	CO
128.53	c	CH
133.45	b	CCl
138.90	a	CC

From the result of ^{1}H and ^{13}C NMR spectra, it can be confirmed that the *p*-Cl-DBS is a product from the reaction of D-sorbitol and 4-chlorobenzaldehyde.

Summary

The chemical structure of sorbitol derivatives (i.e. *o*-Cl-DBS, *m*-Cl-DBS, *p*-Cl-DBS, and *p*-Br-DBS) were characterized by FT-IR and ^{1}H-NMR spectroscopy. The result of both techniques can confirm that all of derivatives are products from reaction of D-sorbitol and aromatic benzaldehyde.

Gel formation and fibril morphology

Wilder and co-workers [49, 65] investigated the morphology of DBS in polymers by using transmission electron microscopy. It was found that the DBS molecule can form highly connected networks, with nanofibrils measure about 10 to 70 nm in diameter and length are up to 500 nm. Therefore, it is interesting to study the morphology of DBS derivatives by using halogen atom substituted into the *ortho*, *meta* and *para* positions of DBS molecule.

The physical gel of sorbitol derivatives were prepared by dissolving various concentrations (0.05-0.2 % wt) in dodecane and tetradecane at elevated temperature until the mixture become a clear solution. After that the homogeneous solution was

cooled down to room temperature. SEM and TEM techniques were used to investigate the fibril morphology of sorbitol derivatives.

SEM micrographs of each sample are shown in Figure 30. It can be seen that the fibril morphology of o-Cl-DBS can be observed with 2 drops of extracted gel 0.2 % wt in organic solvents. Fibril morphology of p-Cl-DBS and p-Br-DBS can be observed with 2 drops of extract gel 0.05 % wt in organic solvents as seen in Figure 30a and 30b. On the other hand, the fibril morphology m-Cl-DBS (Figure 30c and 30d) with 1 drop of extracted gel from 0.2 % wt in organic solvents reveals dense fibrils and merge together. Therefore the dimensional and length of fibril of m-Cl-DBS cannot be measured.

From the result above, the fibrils of p-Cl-DBS and p-Br-DBS can be observed at lower concentration than that of o-Cl-DBS. Since the concentration is higher than 0.05 % wt, the fibrils are thick and not easy to observed. The fibrils of o-Cl-DBS in SEM micrographs (Figure 30a and 30b) are flatter and bigger than that of p-Cl-DBS and p-Br-DBS (Figure 30e-30h).

For TEM micrographs of gel extracted from 0.1 % wt of o-Cl-DBS and m-Cl-DBS and 0.05 % wt of p-Cl-DBS and p-Br-DBS are shown in Figure 31. It reveals that the gel extracted of sorbitol derivatives in alkanes are in the form of fibril bundle and twisted.

Sample	Solvent	
	Dodecane	**Tetradecane**
0.2%w/v **o-Cl-DBS**	a	b
0.2%w/v **m-Cl-DBS**	c	d
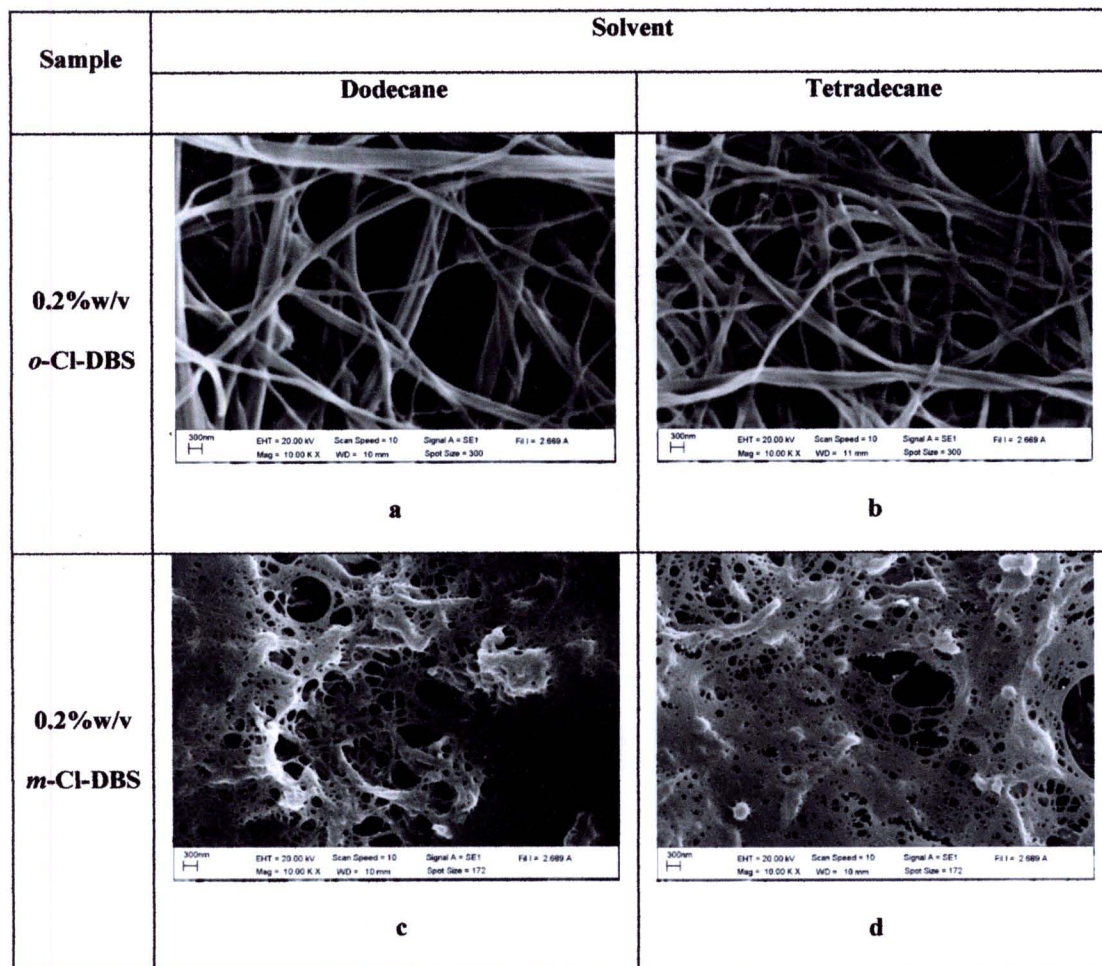
Figure 30 SEM micrographs of sorbitol derivatives in different concentrations and solvents

Sample	Solvent	
	Dodecane	**Tetradecane**
0.05%w/v **_p_-Cl-DBS**	 e	 f
0.05%w/v **_p_-Br-DBS**	 g	 h
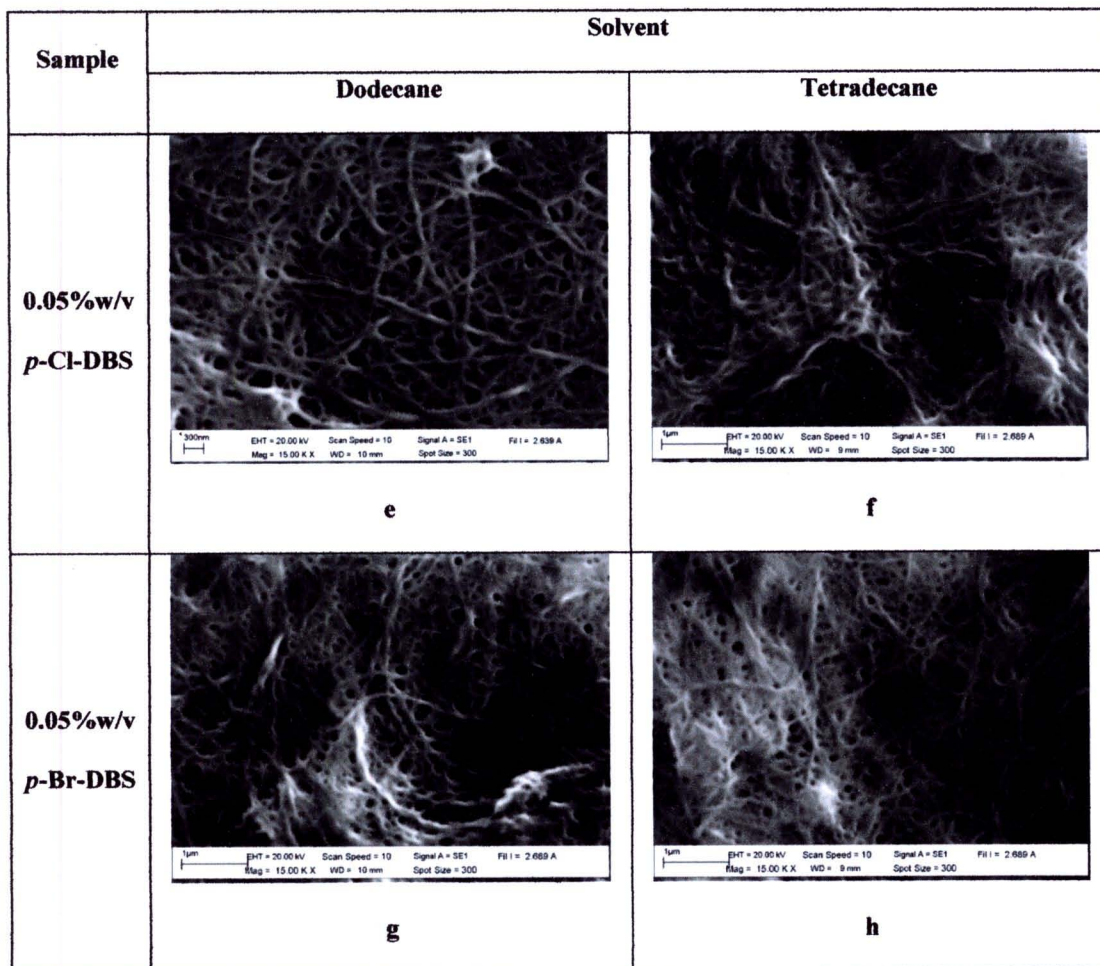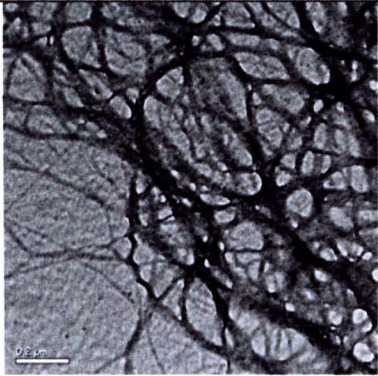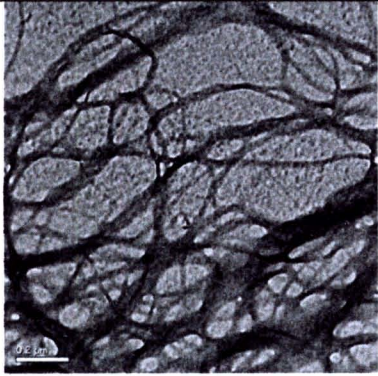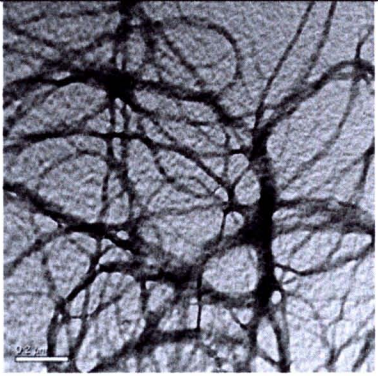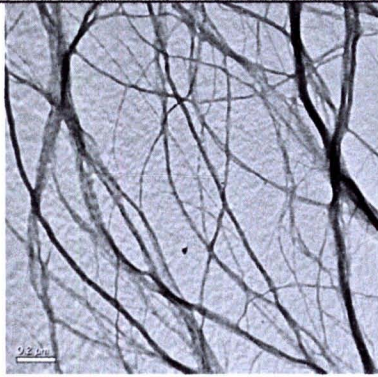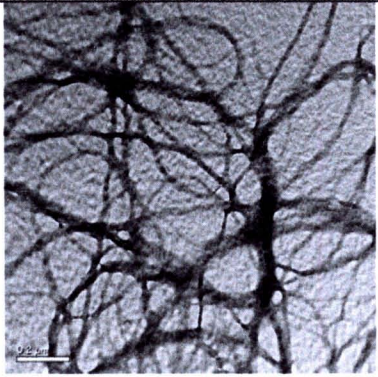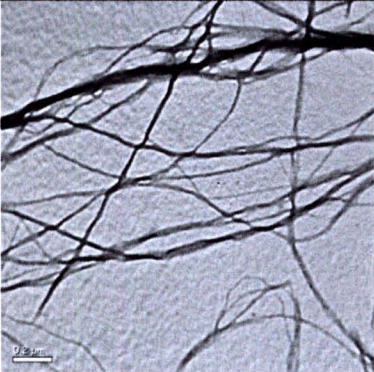
Figure 30 (Cont.)

Sample	Solvent	
	Dodecane	Tetradecane
0.1%w/v *o*-Cl-DBS	 a	 b
0.1%w/v *m*-Cl-DBS	 c	 d
0.05%w/v *p*-Cl-DBS	 e	 f

Figure 31 TEM micrographs of sorbitol derivatives in different concentrations and solvents

Sample	Solvent	
	Dodecane	Tetradecane
0.05%w/v *p*-Br-DBS	g	h

Figure 31 (Cont.)

Table 11 and Table 12 show the dimension of gel extracted of sorbitol derivatives observed by SEM and TEM techniques. It can be observed that the diameter of observed fibrils are varied from 14 to 216 nm and their length are more than 7 μm for 0.1 and 0.2 % wt of *o*-Cl-DBS. The diameters of *m*-Cl-DBS fibrils at 0.1 % wt are in the range of 15 to 33 nm. For 0.05 % wt of *p*-Cl-DBS, fibrils lengths are more than 9 μm and diameters are varied from 7 to 90 nm. At 0.05 % wt of *p*-Br-DBS sample length are more than 7μm and diameter are varied from 10 to 150 nm. It can be seen that the diameters and length of *p*-Cl-DBS and *p*-Br-DBS fibrils were slightly different.

Table 11 Diameter and length of sorbitol derivatives observed by SEM technique

Sample	Diameter (nm)	Length (μm)
0.2%wt *o*-Cl-DBS in tetradecane	46 - 216	> 7
0.2%wt *o*-Cl-DBS in dodecane	79 - 214	> 7
0.2%wt *m*-Cl-DBS in tetradecane	30 - 46	> 7
0.2%wt *m*-Cl-DBS in dodecane	30 - 49	> 7
0.05%wt *p*-Cl-DBS in tetradecane	50 - 80	> 9
0.05%wt *p*-Cl-DBS in dodecane	50 - 90	> 7
0.05%wt *p*-Br-DBS in tetradecane	50 - 150	> 7
0.05%wt *p*-Br-DBS in dodecane	30 - 120	> 7

Table 12 Diameter of sorbitol derivatives observed by TEM technique

Sample	Diameter (nm)
0.10%wt *o*-Cl-DBS in tetradecane	19 - 33
0.10%wt *o*-Cl-DBS in dodecane	14 - 29
0.10%wt *m*-Cl-DBS in tetradecane	15 - 24
0.10%wt *m*-Cl-DBS in dodecane	19 - 33
0.05%wt *p*-Cl-DBS in tetradecane	16 - 70
0.05%wt *p*-Cl-DBS in dodecane	7 - 23
0.05%wt *p*-Br-DBS in tetradecane	10 - 27
0.05%wt *p*-Br-DBS in dodecane	13 - 30

Dodecane and tetradecane were used as solvent for sample preparation. It is likely that the different lengths of alkane have no effect on diameter and length of these fibrils. In case of 0.05 % wt of *o*-Cl-DBS and *m*-Cl-DBS samples, the fibril network could not be observed by TEM technique. Therefore, the concentration of *o*-Cl-DBS and *m*-Cl-DBS were increased up to 0.1 % wt. As the amount of *o*-Cl-DBS and *m*-Cl-DBS increased, the fibril network can be clearly seen. However, their diameters are similar to those of *p*-Cl-DBS and *p*-Br-DBS.

Summary

SEM and TEM micrographs of gel extracted from organic solvent revealed the fibril network of chloro and bromo substitutes which their diameters can be observed in the range of 7-216 nm and length higher than 9 μm.

The effect of sorbitol derivatives on crystallization, melting temperature, degree of crystallinity and nucleation of polypropylene

In this topic, the effect of sorbitol derivatives on crystallization, melting temperature and degree of crystallinity of polypropylene (in term of amount, substitution position, and type of sorbitol derivatives) are studied by using Differential Scanning Calorimeter (DSC, Mettler Toledo DSC1). The samples prepared by solution and melt-blending, were heated from 25 °C to 180 °C with a heating rate of 10 °C/min, and then cooled down from 180 °C to 25 °C with a cooling rate of 5 °C/min, and reheated from 25 °C to 180 °C with a heating rate of 10 °C/min. Furthermore, the samples from melt-blending were melted at 210 °C for 2 minutes then crystallized at 130 °C for 30 minutes for study the effect of sorbitol derivatives on nucleation of polypropylene crystals.

The effect of sorbitol derivatives on crystallization temperature of polypropylene

The crystallization temperature of neat iPP and iPP containing sorbitol derivatives were shown in Figure 32. The onset and peak temperatures in the thermogram indicate to the initial temperature where the crystallization begin and the minimum temperature where maximum crystallization occurred, respectively. From cooling thermogram, the shoulder was found in the case of iPP containing 0.1 % wt of *p*-Cl-DBS and *p*-Br-DBS. This suggests that the samples have different sizes of sperulites. It is due to the dispersion of *p*-Cl-DBS and *p*-Br-DBS are not good enough during mixing.
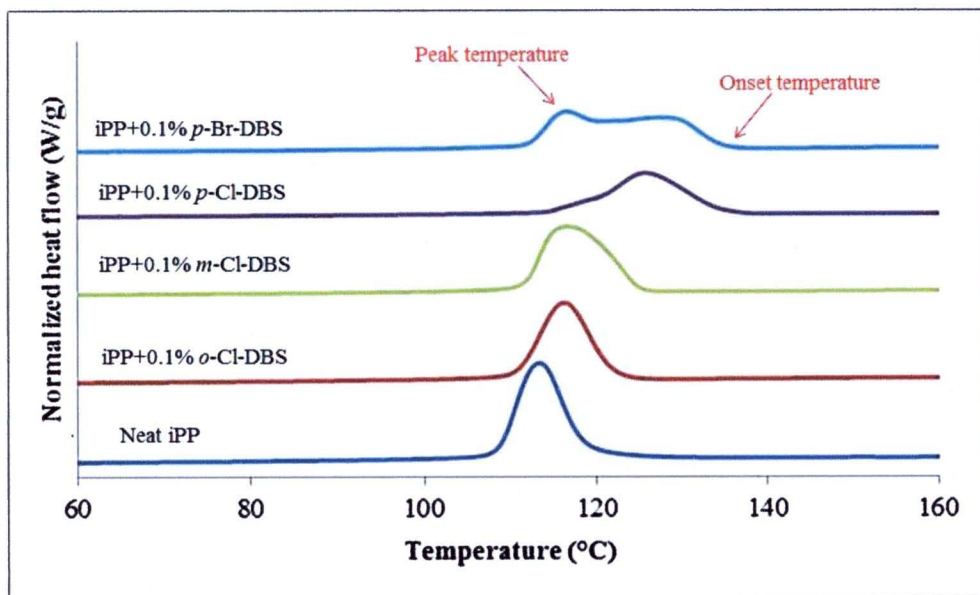
Figure 32 Cooling thermograms of neat iPP and iPP containing 0.1 % wt of sorbitol derivatives by solution blending
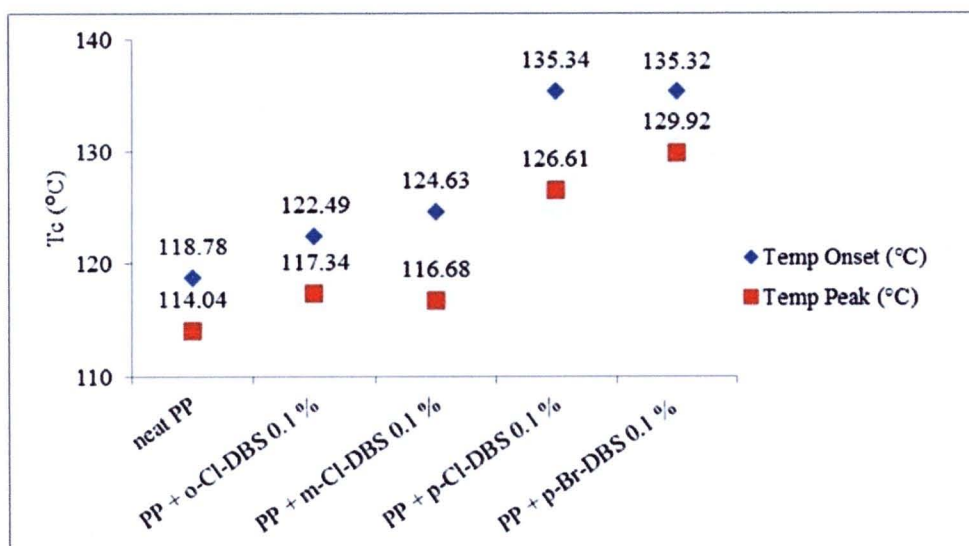
Figure 33 Crystallization temperature of neat iPP and iPP containing 0.1%wt of sorbitol derivatives by solution blending

The iPP samples with the same amount of Cl-DBS were investigated in term of substitution position. It was found that *p*-Cl-DBS shows the highest crystallization temperature (T_c) of iPP as seen in Figure 33. The effect of type of sorbitol derivatives (bromo and chloro substitution) on the crystallization temperature (T_c) of iPP was not much different. Both derivatives show an increasing of crystallization temperature (T_c) of iPP to about 20 °C compared to neat iPP.
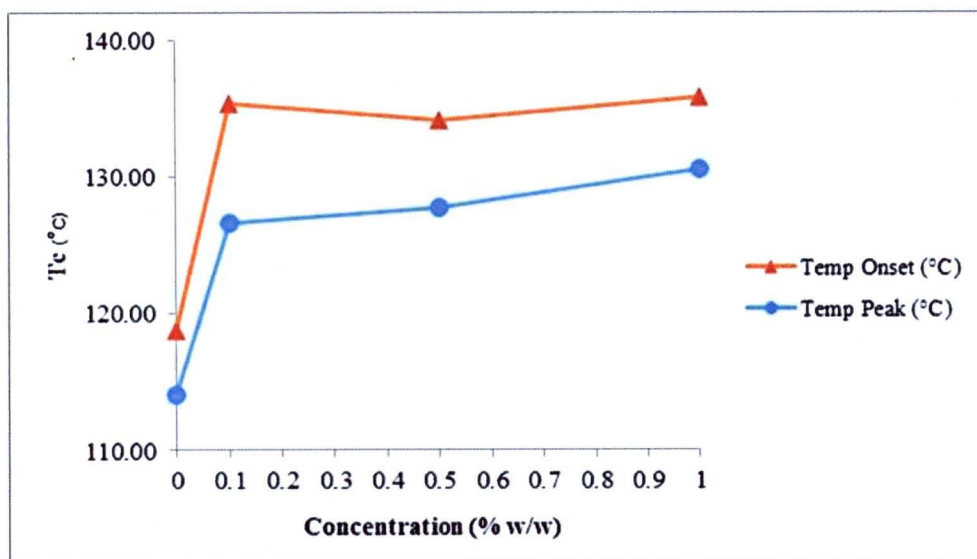
Figure 34 Crystallization temperature of neat iPP and iPP containing different concentration of *p*-Cl-DBS by solution blending

Different amounts of *p*-Cl-DBS in iPP sample were investigated in term of crystallization temperature (T_c) of iPP (Figure 34). It was found that adding 0.1 %wt of *p*-Cl-DBS increase the crystallization temperature (T_c) of iPP up to 17 °C compared to neat iPP. At concentration higher than 0.1 %wt, it is likely that crystallization temperature (T_c) of iPP contained *p*-Cl-DBS remains constant. This is due to the excess amount of nucleating agent to act as a nucleating agent for iPP. The densities of nuclei are not contributing nucleation effect faster than this. Since solution blending technique gives a small amount of sample, it is not enough for the next process. So, the samples will be needed to prepare by two-roll mill technique.
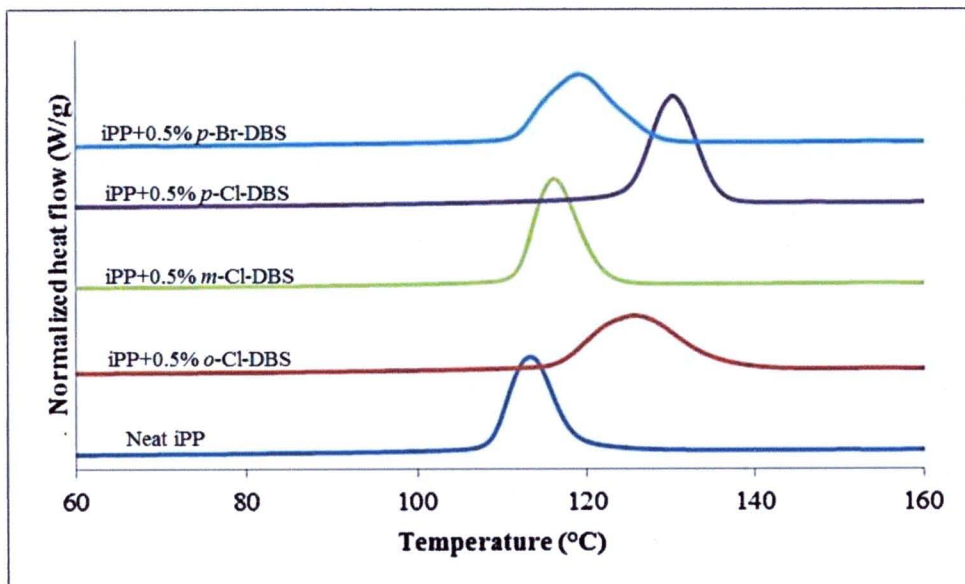
Figure 35 Cooling thermograms of neat iPP and iPP containing 0.5 %wt of sorbitol derivatives by two-roll mill

Table 13 Crystallization temperature of neat iPP and iPP containing 0.5 %wt of sorbitol derivatives

Sample	Crystallization temperature (°C)	
	Onset	Peak
Neat iPP	118.78	114.04
iPP/0.5%o-Cl-DBS	133.24	124.59
iPP/0.5%m-Cl-DBS	122.52	117.46
iPP/0.5%p-Cl-DBS	136.42	131.61
iPP/0.5% p-Br-DBS	127.99	114.04

Figure 35 and Table 13 show cooling thermogram of crystallization temperature (T_c) of iPP and iPP containing the same amount of chloro derivatives (0.5 % wt) by two-roll mill. It can be seen that o-Cl-DBS and p-Cl-DBS show more effective in term of increasing the crystallization temperature (T_c) of iPP. In term of type, the chloro derivatives show an increasing in the crystallization temperature of iPP more than bromo derivative.
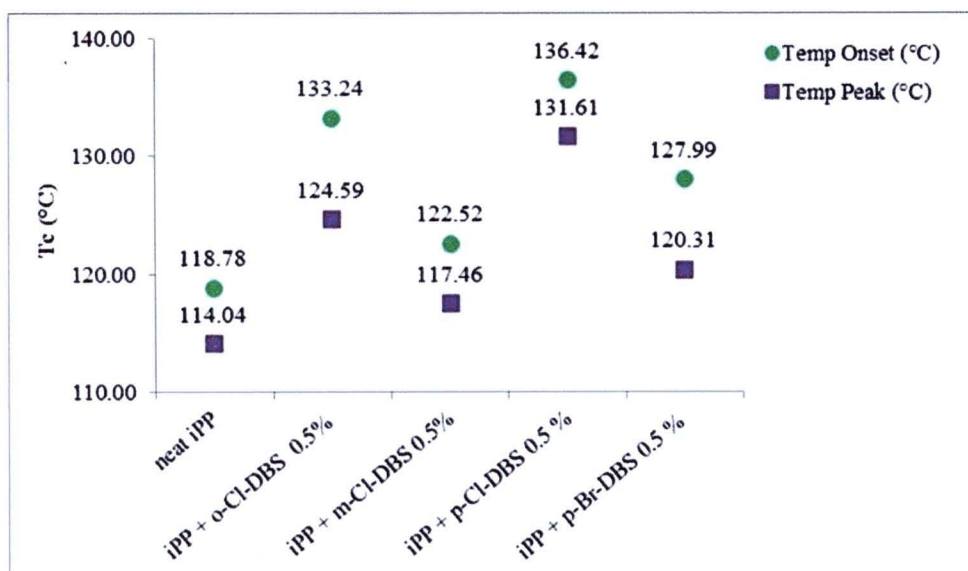
Figure 36 Crystallization temperature of neat iPP and iPP containing 0.5 %wt of sorbitol derivatives by two-roll mill

The influence of different substitution positions and type of sorbitol derivatives on crystallization temperature (T_c) are shown in Figure 36. It can be observed that the p-Cl-DBS show the most effective in term of increasing the crystallization temperature (T_c) of iPP compared to neat iPP and iPP containing the other derivatives at the same concentration.

The cooling thermogram of neat iPP and iPP containing different concentrations of p-Cl-DBS by two-roll mill were shown in Figure 37. It can be seen that the addition of 0.5 %wt of p-Cl-DBS increases the crystallization temperature (T_c) of iPP. At concentration higher than 0.5 %wt, it is likely that the crystallization temperature (T_c) of iPP contained p-Cl-DBS remain constant as shown in Figure 38.
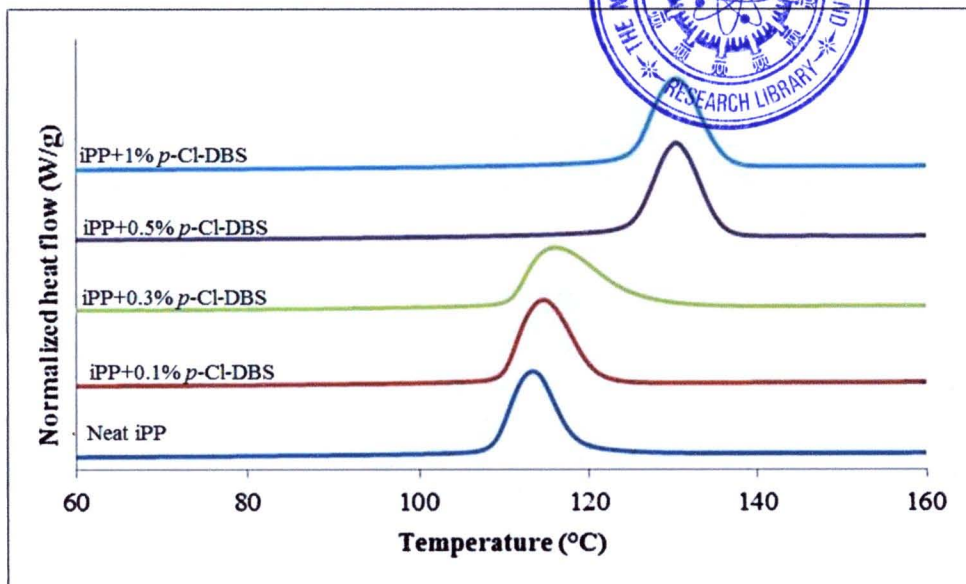
Figure 37 Cooling thermograms of neat iPP and iPP containing different concentrations of *p*-Cl-DBS by two-roll mill
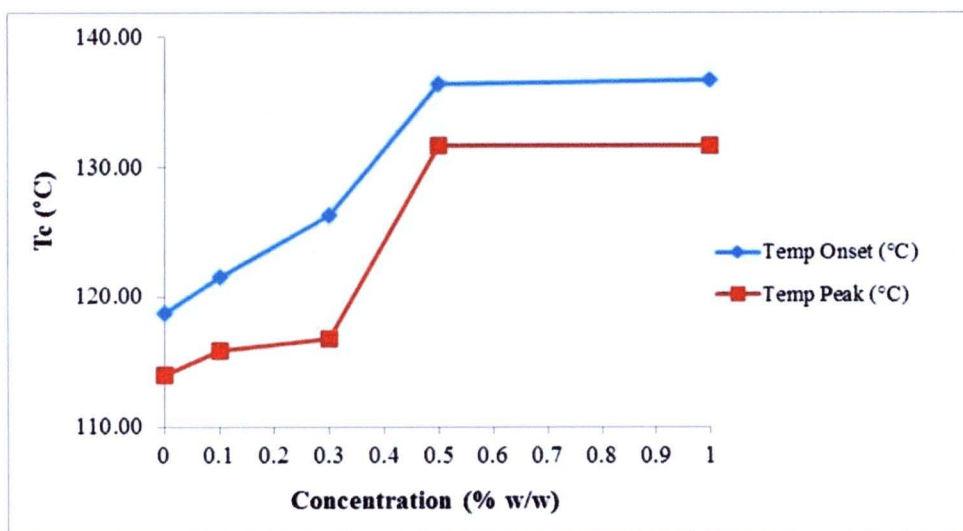
Figure 38 Crystallization temperature of neat iPP and iPP containing different concentrations of *p*-Cl-DBS by two-roll mill

The effect of sorbitol derivatives on melting temperature of polypropylene

Figure 39 shows the melting thermograms of neat iPP and iPP containing different concentrations of p-Cl-DBS. The effect of amount of sorbitol derivatives on the melting temperature (T_m) of iPP was shown in Figure 40. It was found that the melting temperature (T_m) observed of p-Cl-DBS in iPP remain more or less constant with various amount of additives.
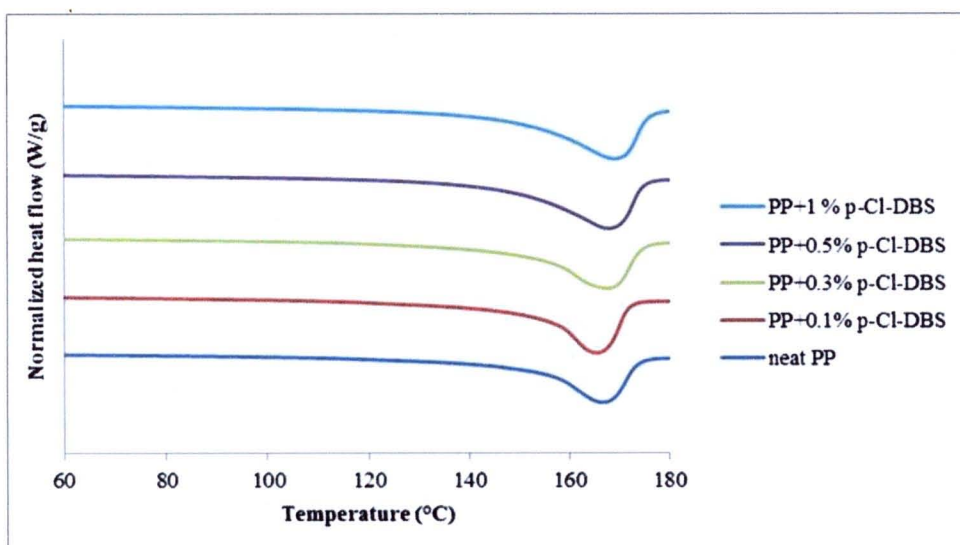
Figure 39 Melting thermograms of neat iPP and iPP containing different concentrations of p-Cl-DBS
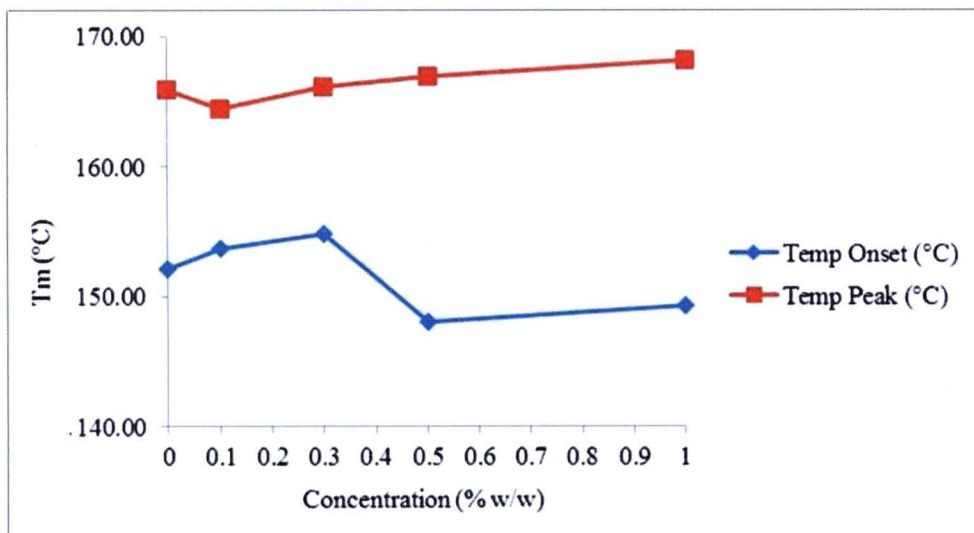
Figure 40 Melting temperatures of neat iPP and iPP containing different concentrations of *p*-Cl-DBS

The data in Figure 41 derived from the second heating thermograms of neat iPP and iPP containing 1 %wt of sorbitol derivatives. The samples were heated and cooled in the same condition as shown in Figure 39. It can be seen that the addition of 1 % wt of sorbitol derivatives are not effecting on the melting temperature of iPP.
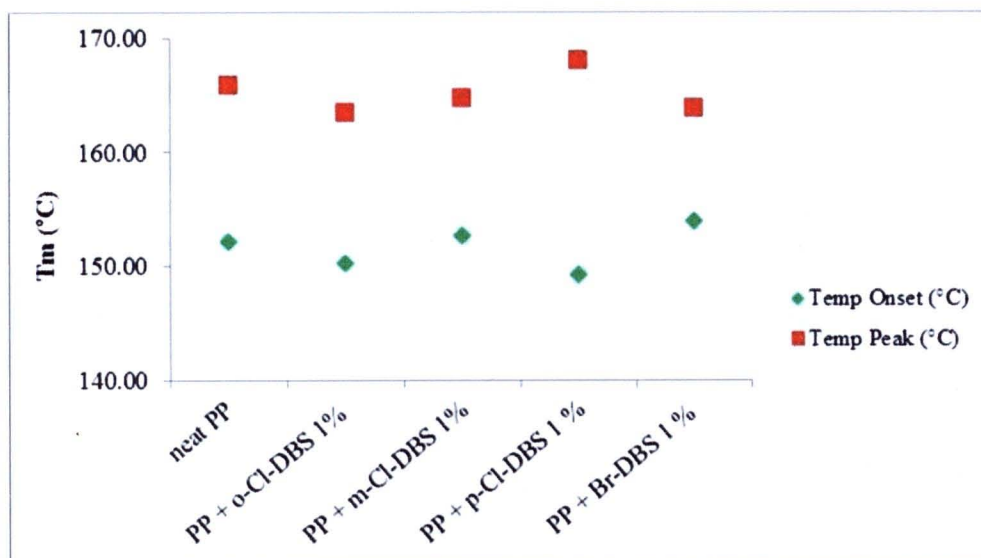
Figure 41 Melting temperatures of neat iPP and iPP containing 1% wt of sorbitol
derivatives

The effect of sorbitol derivatives on the degree of crystallinity of
polypropylene

The effect of sorbitol derivatives on the degree of crystallinity of iPP were
studied from the second heating thermogram of neat iPP and iPP containing sorbitol
derivatives by DSC technique. This is due to the samples were treated under the same
thermal treatment. The degree of crystallinity of neat iPP and iPP containing sorbitol
derivatives were calculated from endothermic enthalpy (second heating) of the sample
(ΔH_{iPP}) where the endothermic enthalpy of the 100 % crystalline PP (ΔH°_{iPP} = 207 J/g
[66])

$$\% \text{ crystallinity} = \Delta H_{iPP} / \Delta H^{\circ}_{iPP} \times 100$$

Table 15 shows the degree of crystallinity of neat iPP and iPP containing 0.5
%wt of sorbitol derivatives. It was found that the degrees of crystallinity of iPP
containing sorbitol derivatives are not changed from the neat iPP. The addition of 0.5
%wt of different substitution positions and types into iPP did not give much affect to
the degree of crystallinity of iPP.

Table 14 Degree of crystallinity of neat iPP and iPP containing 0.5% wt of sorbitol derivatives

Sample	Heating	$\Delta H_{f,PP}$ (J/g)	% crystallinity
Neat iPP	Second	95.94	46.33
iPP/0.5%o-Cl-DBS	Second	106.11	51.24
iPP/0.5%m-Cl-DBS	Second	102.13	49.31
iPP/0.5%p-Cl-DBS	Second	107.78	52.04
iPP/0.5%p-Br-DBS	Second	101.61	49.06

The degree of crystallinity of iPP with different amounts of p-Cl-DBS shown in Table 16, it was found that the addition of 0.5 % wt of p-Cl-DBS increase the degree of crystallinity of iPP. This is correlated with the crystallization temperature (Tc) at 0.5 % wt of p-Cl-DBS. This corresponds to the higher rate of nucleation and growth of crystalline, the greater degree of crystallinity.

Table 15 Degree of crystallinity of neat iPP and iPP containing different concentrations of p-Cl-DBS

Sample	Heating	$\Delta H_{f,PP}$ (J/g)	% crystallinity
Neat iPP	Second	95.94	46.33
iPP/0.1%p-Cl-DBS	Second	101.85	49.18
iPP/0.3%p-Cl-DBS	Second	102.02	49.26
iPP/0.5%p-Cl-DBS	Second	107.78	52.04
iPP/1.0%p-Cl-DBS	Second	102.38	48.95

The comparison of the degree of crystallinity between compressed sample (Table 16) and as-spun fiber (Table 17) was investigated. It was found that the degrees of crystallinity of as-spun iPP fibers are higher than that of compressed sample. Since the crystallization under shear flow by extruder, the polymer chains are oriented in the melt, this makes the higher nucleation density when compared to the crystallization under static condition.

Table 16 Degree of crystallinity of as-spun neat iPP fiber and as-spun iPP containing different concentrations of *p*-Cl-DBS fiber

Sample	Heating	$\Delta H_{f,PP}$ (J/g)	% crystallinity
Neat iPP	Second	153.59	74.16
iPP/0.1%*p*-Cl-DBS	Second	153.27	74.02
iPP/0.3%*p*-Cl-DBS	Second	154.77	74.73
iPP/0.5%*p*-Cl-DBS	Second	153.55	74.14
iPP/1.0%*p*-Cl-DBS	Second	146.87	70.92

The effect of amount of *p*-Cl-DBS on the degrees of crystallinity of as-spun fiber is shown in Table 17. It can be observed that the degrees of crystallinity of iPP containing different concentration of *p*-Cl-DBS fiber are not changed when compared to neat iPP fiber.

The effect of sorbitol derivatives on nucleation of polypropylene

The crystallization of polymer has two consecutive steps: nucleation and growth of crystals. The nucleation can be either homogeneous or heterogeneous nucleation [28]. Homogeneous nucleation does not contain foreign particles inside which can cause nucleation. Heterogeneous nucleation occurs when there are foreign particles inside which can cause an increase in rate of crystallization. In this work, the sorbitol derivatives were used as a foreign to nucleate crystallization of polypropylene. The effect of sorbitol derivatives on spherulite size of iPP were observed by optical microscopy technique. Figure 42 shows spherulite structures of neat iPP and iPP containing sorbitol derivatives. Figure 42a demonstrates the spherulite structures of neat iPP which, was clearly seen. The addition of 0.1 % wt of sorbitol derivatives into iPP was not clearly seen the different of spherulite size, but it is smaller than that of neat iPP (as shown in Figure 42b - 42e).
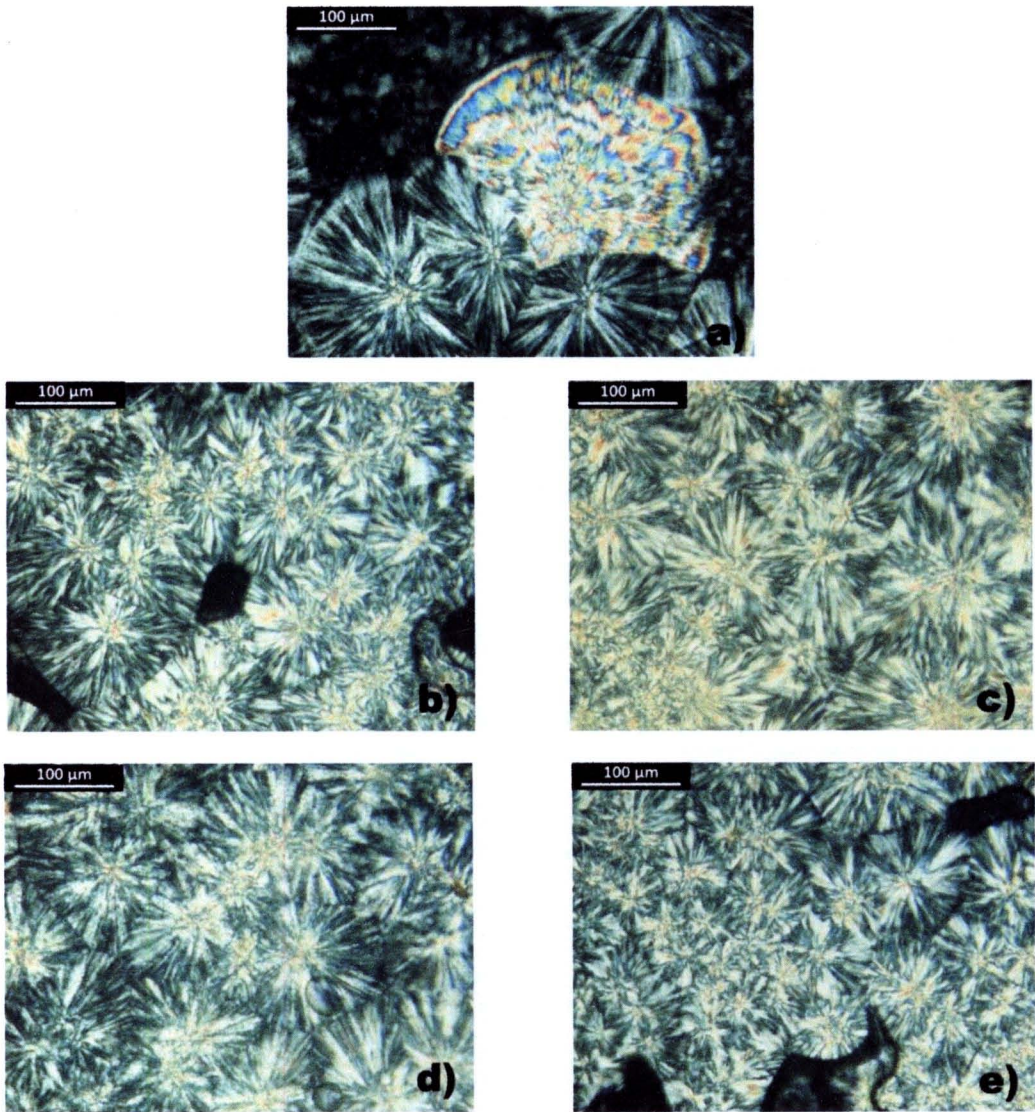
Figure 42 Optical micrographs of a) neat iPP b) iPP/0.1%*o*-Cl-DBS c) iPP/ 0.1%*m*-Cl-DBS d) iPP 0.1%*p*-Cl-DBS and e) iPP/0.1%*p*-Br-DBS from melt-blend

Since it is not clearly seen the effect or nucleating on iPP when the amount of derivatives are low. Figure 43 shows optical micrographs of iPP containing 0.5 % wt of sorbitol derivatives, it is likely that the spherulite sizes of iPP are smaller than iPP contained 0.1% wt of all sorbitol derivatives. While partial spherulite structures of iPP containing 0.5 % wt of *o*-Cl-DBS and *m*-Cl-DBS still be visible large sizes. On the

contrary, the addition of 0.5% wt of *p*-Cl-DBS and *p*-Br-DBS (Figure 43c and 43d) show a very dramatic decreasing in spherulite sizes of iPP corresponding to the result from DSC. Especially the spherulit sizes of iPP containing 0.5% wt of *p*-Br-DBS (Figure 43d) are very small and regular compared to the other derivatives. The *p*-Br-DBS indicates the most effectiveness in acting as a nucleating agent for iPP compared to the others. This result is consistent with the crystallization temperature and degree of crystallinity of iPP as mentioned above. Meanwhile, this is similar to the studying of Kristainsen [10] by adding 0.2-1% wt of DMDBS in iPP for study optical property.
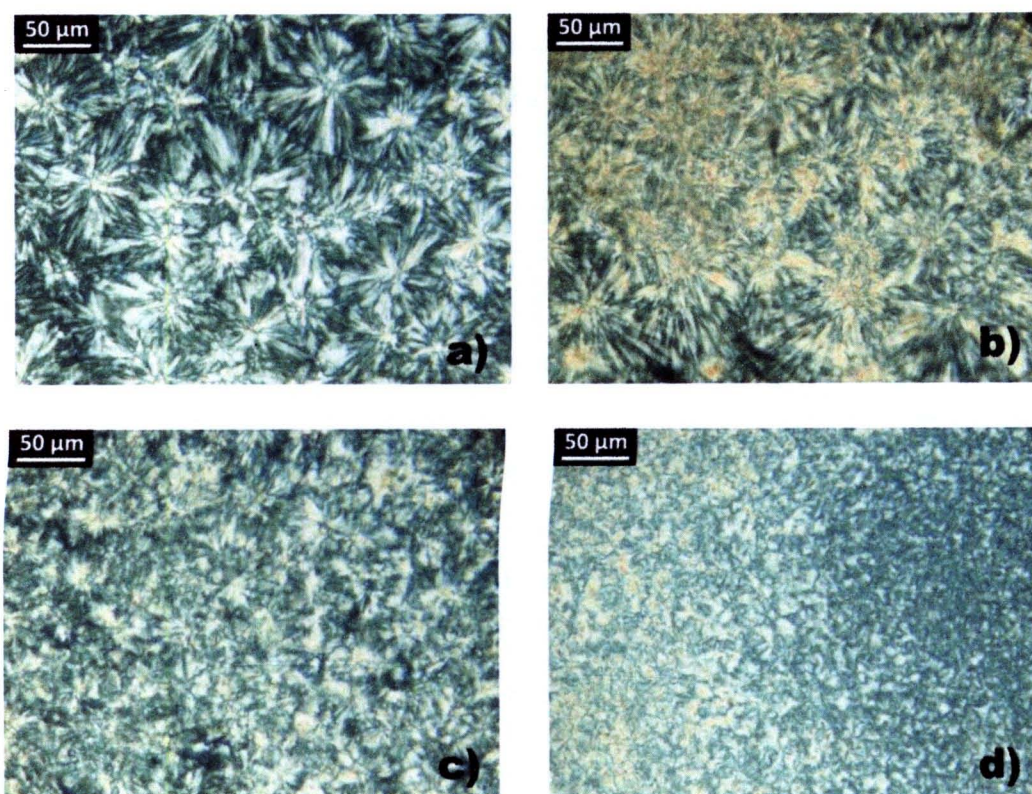
Figure 43 Optical micrographs of iPP containing 0.5% wt of a) *o*-Cl-DBS, b) *m*-Cl-DBS, c) *p*-Cl-DBS and d) *p*-Br-DBS from melt-blend

Summary

The effect of sorbitol derivatives on the crystallization of iPP were studied using different scanning calorimeter technique (DSC). It was found that addition of small amount of sorbitol derivative increase the crystallization temperature of iPP to 18 °C compared to neat iPP. No further increase in the crystallization temperature when the amount of additive reach 0.5 wt% for *para* chloro derivatives. The *para* chloro substitution indicates that the most effective among the other derivatives to nucleate iPP. DSC studies also showed that derivatives did not change the melting temperature of iPP. The addition of 0.5 % wt of *p*-Cl-DBS increased the degree of crystallinity of iPP 12 % for compressed sample. On the other hand, the additions of p-Cl-DBS more or less are not effective on the degree of crystallinity of iPP fiber.

Optical micrograph of iPP dispersed with 0.1% wt of all sorbitol derivatives showed smaller spherulite size than that of neat iPP. At high concentration (0.5 % wt) of sorbitol derivatives, the addition of *p*-Br-DBS revealed the very dramatic decrease in spherulite sizes of iPP compared to *p*-Cl-DBS, *o*-Cl-DBS, and *m*-Cl-DBS. Therefore, these materials are able to use as a nucleating agent for iPP.

The effect of sorbitol derivatives on the morphology and orientation of polypropylene

In this work, various types and amounts of sorbitol derivatives were dispersed in iPP by using two-roll mill technique. The blend samples were spun into fiber form under the flow field during extrusion process. The sorbitol derivatives act as a nucleating agent and may direct the crystallization of polypropylene crystal. This templating process will give high orientation of polymer crystal. The effect of various types and amounts of sorbitol derivatives on morphology and orientation of iPP will be investigated. The die temperature, screw speed including draw ratio of iPP fiber will also be investigated. The effect of sorbitol derivatives on orientation of iPP fiber will be studied by using SAXS and WAXS techniques. Since semi-crystalline polymers are composed of crystalline and amorphous regions. The distance between the amorphous and crystalline layer is known as the long period or long spacing. The morphology of semi-crystalline polymer is dependent on the crystallization process. The combination of sorbitol derivatives and flow field has a strong effect on the

morphology of iPP. The morphology of iPP and iPP with four different types of sorbitol derivatives will be observed by SEM technique.

The effect of die temperature (T_{die}) on orientation of neat iPP fiber

T_{die} 225 °C		T_{die} 190 °C	
SAXS	WAXS	SAXS	WAXS
a	b	c	d
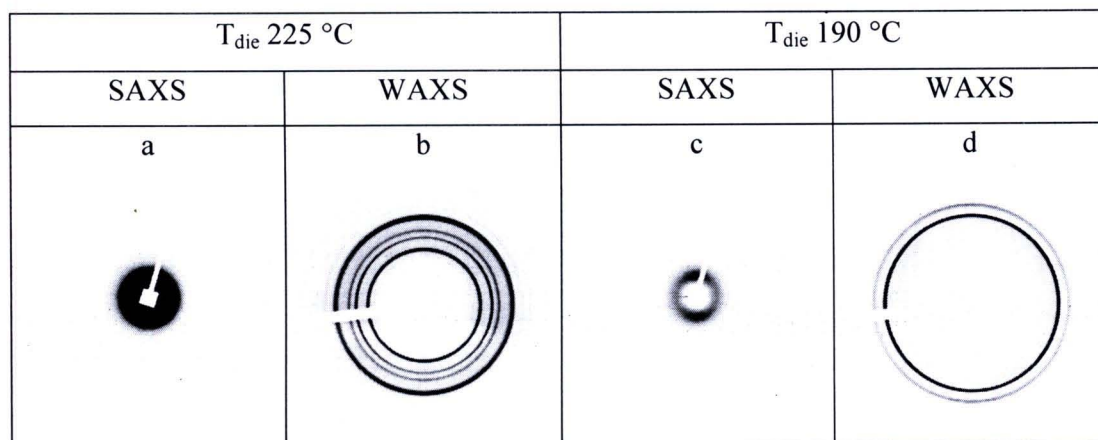
Figure 44 SAXS and WAXS patterns of neat iPP fiber at different die temperatures screw speed 2 rpm

SAXS and WAXS patterns of as-spun neat iPP at die temperature 225 °C in Figure 44a and 44b show no preferred orientation. When the die temperature is decreased (190 °C) WAXS pattern of as-spun neat iPP shows an isotropic distribution of intensity throughout the crystallization. It is indicating that in this condition the crystal are randomly oriented. Conversely, it is clearly seen that the crystal structure is changed as seen in Figure 44b and 44d. While, the SAXS pattern at low die temperature (190 °C) shows low level of preferred orientation (Figure 44c).
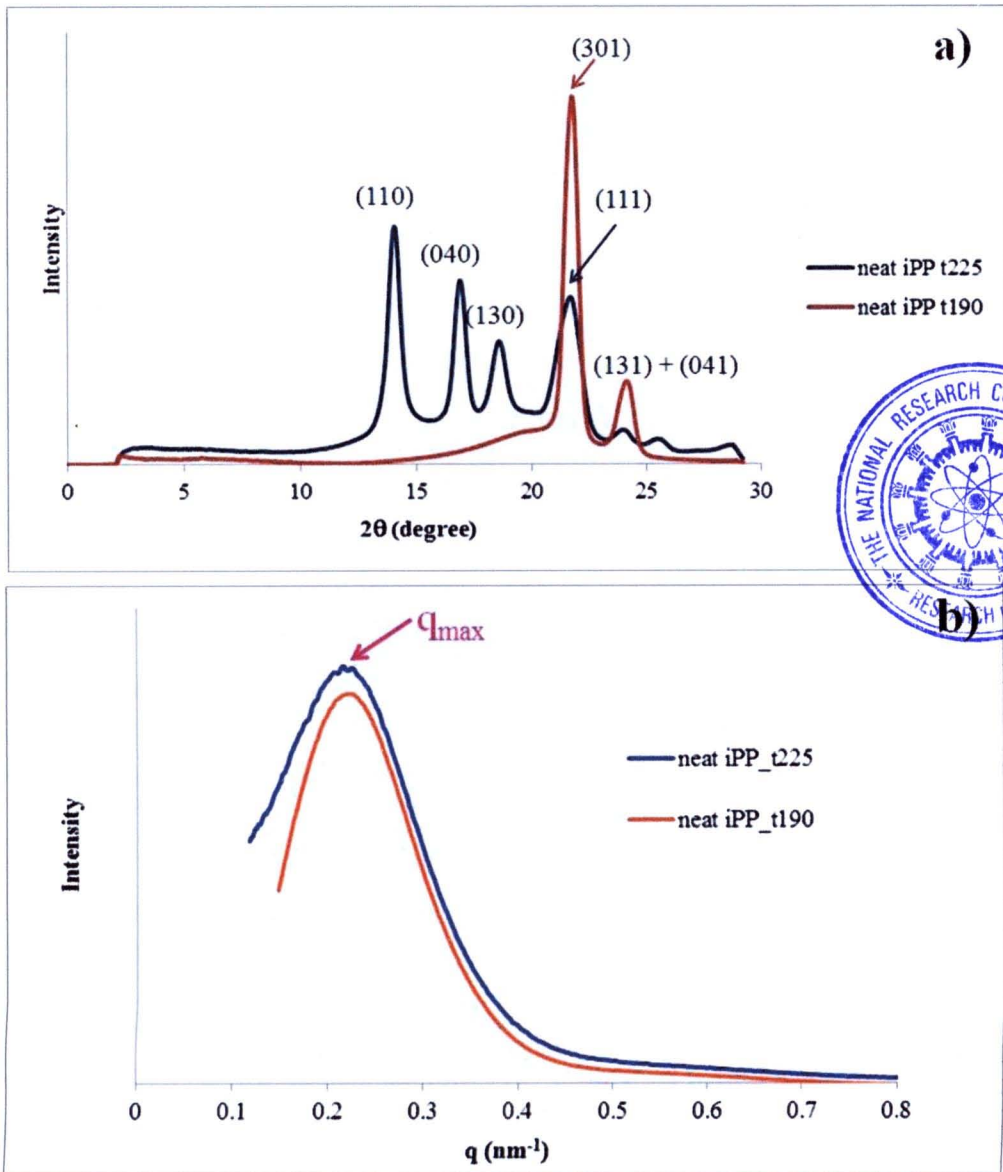
Figure 45 a) Equatorial sections of WAXS patterns, and b) Meridional section of SAXS of neat iPP fiber at different die temperatures
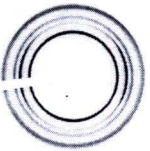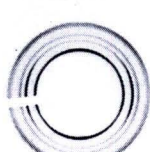
Many researchers demonstrate the oriented crystal development in iPP under shear flow. They found that the diffraction peaks of the monoclinic α-phase at the scattering angles 2θ of 14.1° (110), 16.9°(040), 18.5° (130), 21.3° (111), and 21.8° (131 and 041). The hexagonal β-iPP modification can be observed at the scattering angles 2θ = 16° (300) and 21° (301)   [67, 68, 69, 70, 71, 75].

Figure 45 also presents a plot of scattered intensity as a function of scattering angle (2θ). The crystal modifications of as-spun neat iPP fiber at die temperature 225 °C which were characterized with WAXS correspond to their crystal modifications of research above. In the case of as-spun neat iPP at die temperature 190 °C, this pattern may be the reflection plane (301) (at the scattering angles $2\theta = 21.4°$) of β-phase. This sample could not be clearly identified. It is due to Bragg reflection plane (300) of as-spun neat iPP at die temperature 190 °C absent, while that in sample from the other researches do not. The β-form can be obtained by specific sample preparation conditions, such as the presence of heterogeneous nucleating agents, crystallization in a temperature gradient or crystallization under shear.

Table 17 q- and d-space of iPP as-spun fiber at different die temperatures at screw speed 2 rpm

T_{die}	q (nm^{-1})	d-space (nm)
225 °C	0.2166	28.9935
190 °C	0.2179	28.8206

Table 17 shows the long period 28.9935 nm of neat iPP ($d = 2\pi/q_{max}$) at die temperatures 225 °C, for die temperature 190 °C the long period is about 28.8206 nm. It demonstrates that the long period of neat iPP in both processing temperatures are not changed. Die temperature indicates no effect on long period of neat iPP. This is similar to study of Kumaraswamy et al. [72]. They examined the influence of shearing condition (examine section along the direction perpendicular to flow, F and along the lobes from the daughter lamellae, D) on the development of semicrystalline morphology in iPP by using in-situ synchrotron X-ray scattering. The value of long spacing (L_B) obtained from an analysis of the F section ($L_{B,F} = 28$ nm) is similar to that from an analysis of the D direction $L_{B,D} = 28.9$ nm.

| Fiber samples	T$_{die}$ 225 °C		T$_{die}$ 190 °C	
	SAXS	WAXS	SAXS	WAXS
iPP+0.5% o-Cl-DBS	a	-	e*	i*
iPP+0.5% m-Cl-DBS	b	-	f	j
iPP+0.5% p-Cl-DBS	c	-	g	k
iPP+0.5% p-Br-DBS	d	-	h	l

* As-spun iPP+0.5% o-Cl-DBS at Tdie 195 °C

- No result (no data)

Figure 46 SAXS patterns of as-spun iPP fiber containing 0.5 % wt of sorbitol derivatives at different die temperatures, and WAXS patterns of as-spun iPP fiber containing 0.5 % wt of sorbitol derivatives at die temperature 190 °C, screw speed 2 rpm

The effect of die temperature and type of sorbitol derivatives were shown in Figure 46. At die temperature 225 °C as-spun iPP containing 0.5 % wt of p-Br-DBS shows low level of lamellar orientation (Figure 46d). When die temperature is decreased the SAXS and WAXS patterns of as-spun iPP with 0.5 % wt of four

different types of sorbitol derivatives (Figure 46g – Figure 46l) demonstrate the high level of lamellar orientation and low preferred orientation of iPP crystal. While, the addition of 1 % wt of *p*-Br-DBS into as-spun iPP at die temperature 225 °C shows the low level of lamellar orientation and low preferred orientation of iPP in SAXS and WAXS patterns, respectively (Figure 49i and Figure 49j). On the other hand, Figure 49k and Figure 49l demonstrate the high level of lamellar orientation and high preferred orientation in SAXS and WAXS patterns, respectively of iPP with 1 % wt of *p*-Br-DBS compared to iPP with 0.5 % wt of *p*-Br-DBS (Figure 46h and Figure 46l) at 190 °C. The die temperature 225 °C indicates no effect on the orientation of iPP with 0.5 and 1 % wt of sorbitol derivatives. It is due to the temperature is too high leading to the sorbitol derivatives can melt in the polymer matrix. Therefore, the sorbitol derivatives are not in the form of fibril thus they could not template the crystallization of iPP.
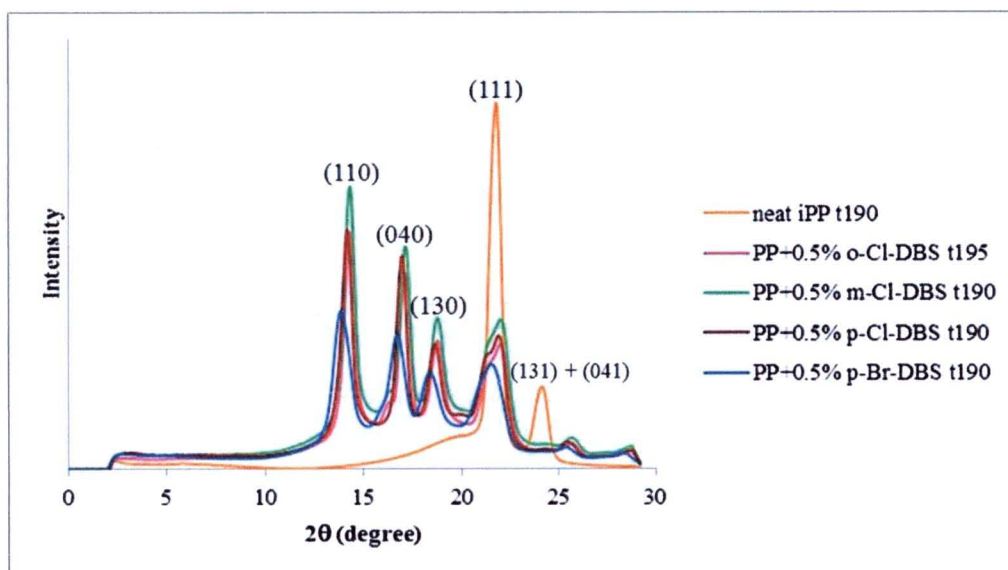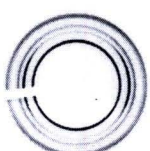

Figure 47 Equatorial sections of WAXS patterns of neat iPP and PP+0.5% wt of sorbitol derivatives at die temperature 190 °C

Figure 47 shows wide-angle X-ray patterns obtained from as-spun neat iPP fiber and iPP fiber containing 0.5 % wt of sorbitol derivatives at die temperature 190 °C. It can be clearly seen that the iPP fiber containing 0.5 % wt of sorbitol derivatives show that the α-crystal reflections, while neat iPP reveals another crystal reflections (it may be β-form). When increase the die temperature up to 225 °C and amount of sorbitol derivatives to 1 % wt, it demonstrates that the WAXS pattern of both neat iPP and iPP fiber containing 1 % wt of sorbitol derivatives are similar as seen in Figure 48.
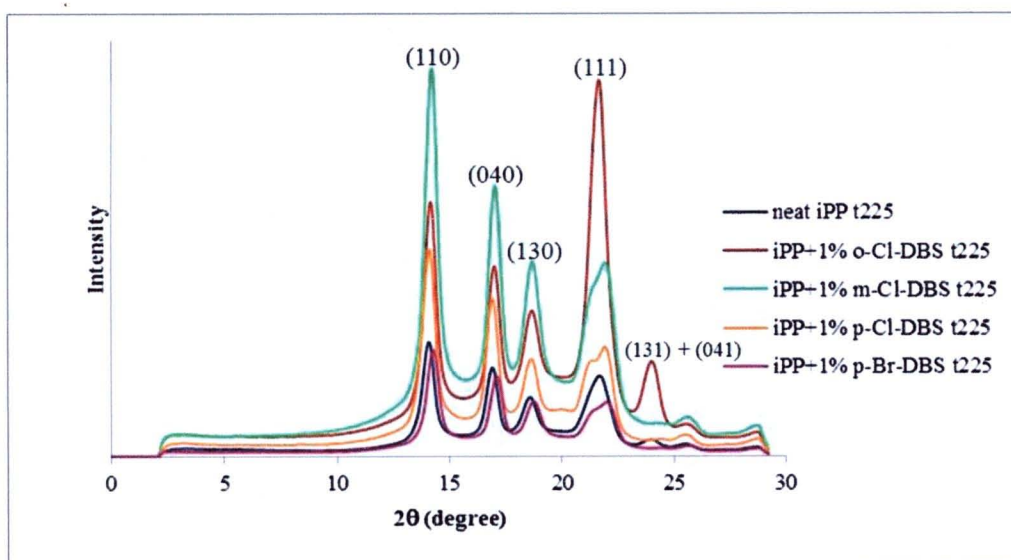
Figure 48 Equatorial sections of WAXS patterns of neat iPP and PP/1% wt of sorbitol derivatives at die temperature 225°C

Fiber samples	T$_{die}$ 225 °C		T$_{die}$ 190 °C	
	SAXS	WAXS	SAXS	WAXS
iPP+1% o-Cl-DBS	a	b	-	-
iPP+1% m-Cl-DBS	c	d	-	-
iPP+1% p-Cl-DBS	e	f	g*	h*
iPP+1% p-Br-DBS	i	j	k	l

* As-spun iPP+1% p-Cl-DBS at Tdie 195 °C

- No result (no data)

Figure 49 SAXS and WAXS patterns of as-spun iPP fiber containing 1 % wt of sorbitol derivatives at different die temperatures and screw speeds

Table 18 q- and d-space of iPP as-spun fiber with small amount of sorbitol derivatives at different die temperatures at screw speed 2 rpm

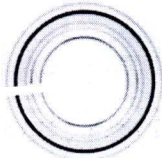| Sample	T_{die} 225 °C		T_{die} 190 °C	
	q (nm^{-1})	d-space (nm)	q (nm^{-1})	d-space (nm)
iPP+0.5% o-Cl-DBS	0.3747	16.7601	0.3648*	17.2149*
iPP+0.5% m-Cl-DBS	0.3747	16.7601	0.3623	17.3337
iPP+0.5% p-Cl-DBS	0.3772	16.6490	0.3137	20.0191
iPP+0.5% p-Br-DBS	0.3847	16.3244	0.3498	17.9531
iPP+1% o-Cl-DBS	0.2166	28.9935	-	-
iPP+1% m-Cl-DBS	0.3822	16.4312	-	-
iPP+1% p-Cl-DBS	0.3050	20.5902	0.3648*	17.2149*
iPP+1% p-Br-DBS	0.3859	16.2736	0.3174	19.7858

* As-spun fiber at Tdie 195 °C

- No result (no data)

The d-spacing of iPP fibers calculated by Bragg's law ($d = 2\pi/q_{max}$) are reported in Table 18. It was found that the d-spacing of as-spun iPP containing 1 % wt of o-Cl-DBS at high die temperature is similar to the long period of as-spun pure iPP at both of processing temperatures. This indicates that 1 % wt of o-Cl-DBS not effective on the long period of iPP. While, the other types of sorbitol derivatives (at same and different conditions) show a decreasing of the long period of iPP. Generally, the long period of polymer were changed by crystallization condition, for example cooling rate and crystallization temperature. Somani [67] reported that the large long period is an indication of loosely packed, lamellae stacks. The long period value does not change with either shear rate or shear duration. This is because the extent of supercooling below the equilibrium temperature.
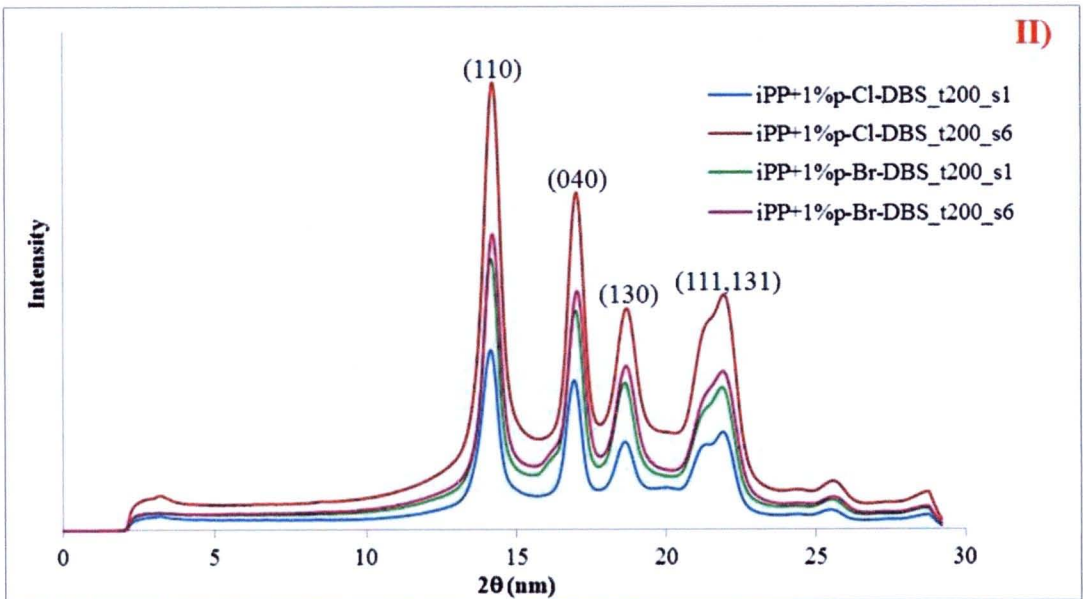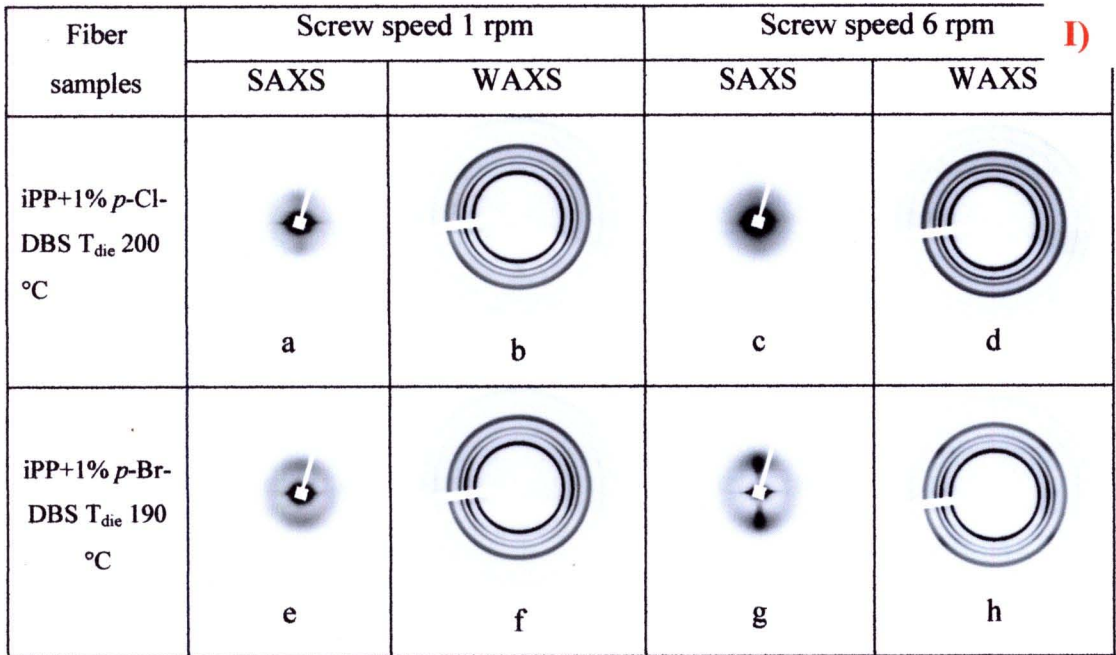
**The effect of screw speed on orientation of neat iPP fiber**

In this topic the effect of different screw speeds at die temperature 190 °C on the orientation of iPP fiber will be studied. Figure 50a and Figure 50b show low level of preferred orientation of iPP crystal in WAXS pattern of neat iPP at different screw speeds.

Fiber sample	Screw speed 1 rpm	Screw speed 6 rpm
Neat iPP	a	b

Figure 50 WAXS patterns of as-spun neat iPP different screw speeds at die temperature 190 °C

Fiber samples	Screw speed 1 rpm		Screw speed 6 rpm	
	SAXS	WAXS	SAXS	WAXS
iPP+1% p-Cl-DBS T_{die} 200 °C	a	b	c	d
iPP+1% p-Br-DBS T_{die} 190 °C	e	f	g	h

I)

II)

Figure 51 I) SAXS and WAXS patterns, II) Equartorial sections of WAXS patterns and III) Meridional section of SAXS of as-spun iPP with 1 % wt of different types of sorbitol derivatives at different screw speeds and die temperatures
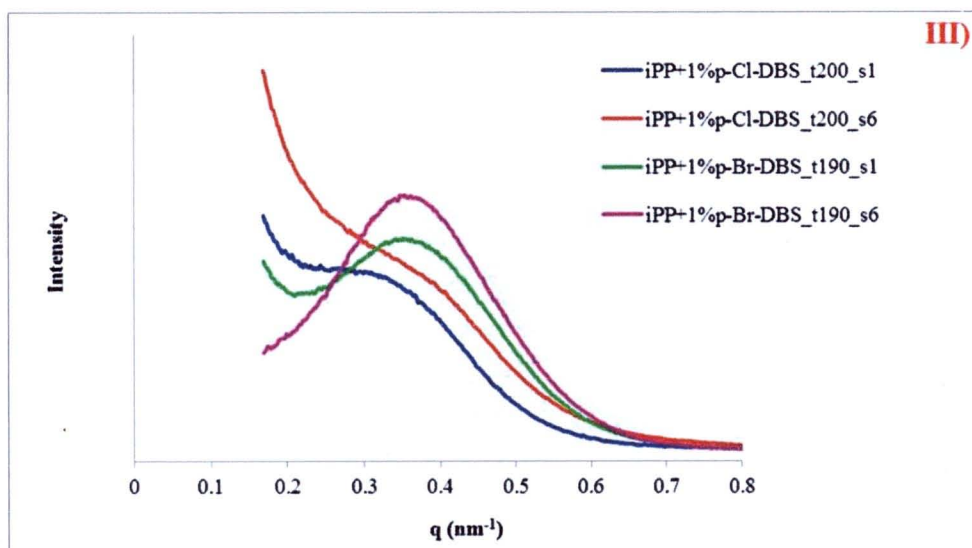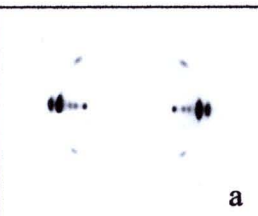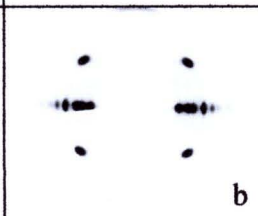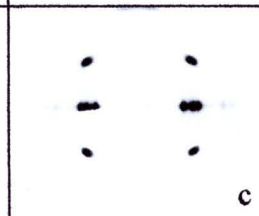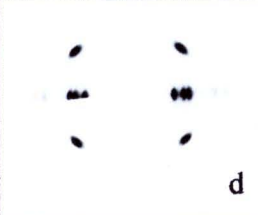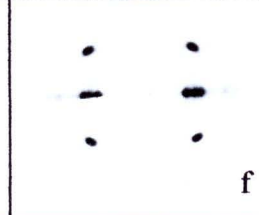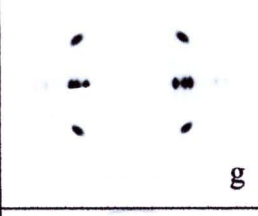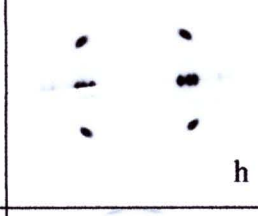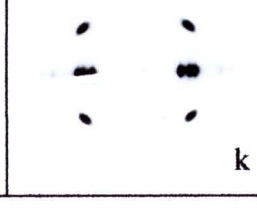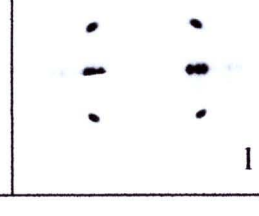
Figure 51 (cont.)

The addition of 1 % wt of *p*-Cl-DBS (Figure 50 a and 50b) at die temperature 200 °C and screw speed 1 rpm and 1% wt *p*-Br-DBS (Figure 51 Ie) and 51 If)) at die temperature 190 °C into iPP fiber are shown the low level of lamellar orientation and low preferred orientation in SAXS and WAXS patterns, respectively. While, at the screw speed 6 rpm of as-spun iPP with 1 % wt of *p*-Cl-DBS show no orientation as seen in Figure 51 Ic) and Figure 51 Id). In contrast, as-spun iPP with 1% wt *p*-Br-DBS demonstrates the high level lamellar orientation of iPP and high level of preferred orientation of iPP crystal.

The high level of lamellar of iPP and iPP crystal are clearly seen when dispersed with small amount of sorbitol derivatives with high shear flow and low processing temperature.

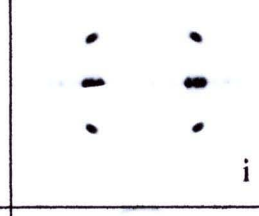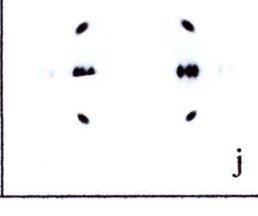**The effect of draw ratio on orientation of drawn fiber neat iPP fiber and drawn fiber iPP with sorbitol derivatives at different draw ratios**

After Neat iPP and iPP/sorbitol derivatives as-spun fiber were prepared, they were continuously fed into a glycerol bath set as 95 °C to draw as-spun fiber. The drawn fibers at minimum to maximum draw ratios were collected by varying the take up velocity.

Sample	Draw ratio 8	Draw ratio 12	Draw ratio 16
Neat at Tdie 225 °C	a	b	c
Neat at Tdie 190 °C	d	e	f
iPP+1%*p*-Cl-DBS at Tdie 190 °C	g	h	i
iPP+1%*p*-Br-DBS at Tdie 190 °C	j	k	l

Figure 52 WAXS patterns of drawn neat iPP fiber at different die temperatures, and iPP fibers containing 1 % wt of sorbitol derivatives at die temperature 190 °C

The crystal orientations of iPP under different draw ratios were shown in Figure 52. Figure 53a) demonstrates the WAXS profiles of drawn neat iPP fiber at die temperature 225 °C with different draw ratios. It can be clearly observed that the crystal orientation of iPP is changed when increasing draw ratio. While, WAXS profiles of drawn neat iPP fiber and iPP containing 1% wt of sorbitol derivatives at die temperature 190 °C show similar crystal orientation of iPP.

The WAXS pattern reveals that the crystal orientation is unaffected by the presence of sorbitol derivatives as seen in Figure 53c) and Figure 53d). It is due to the structure of iPP was changed during the drawn fiber process.
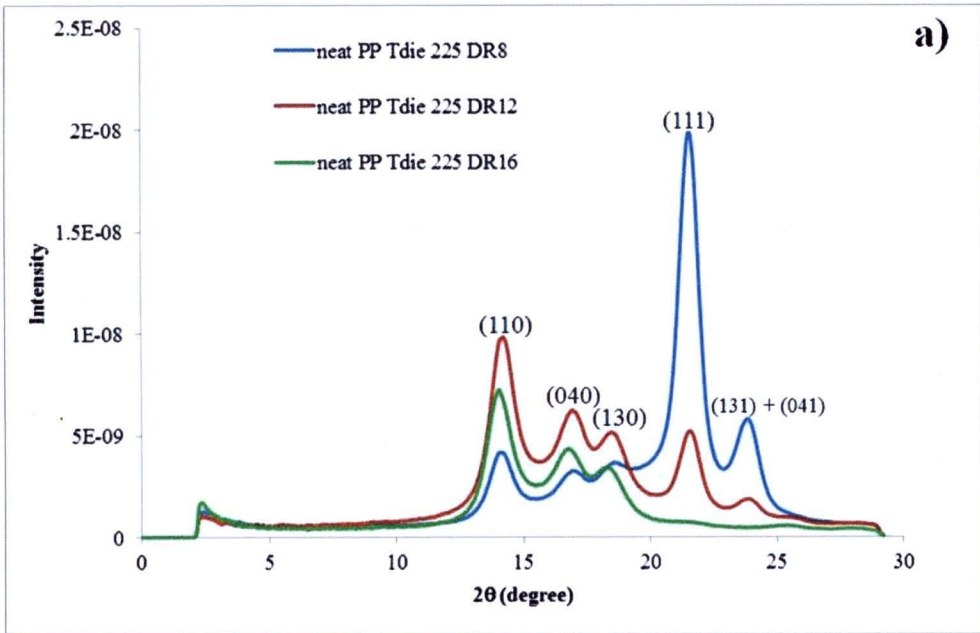
Figure 53 a) Equatorial section of drawn neat iPP fiber at die temperature 225 °C with different draw ratios
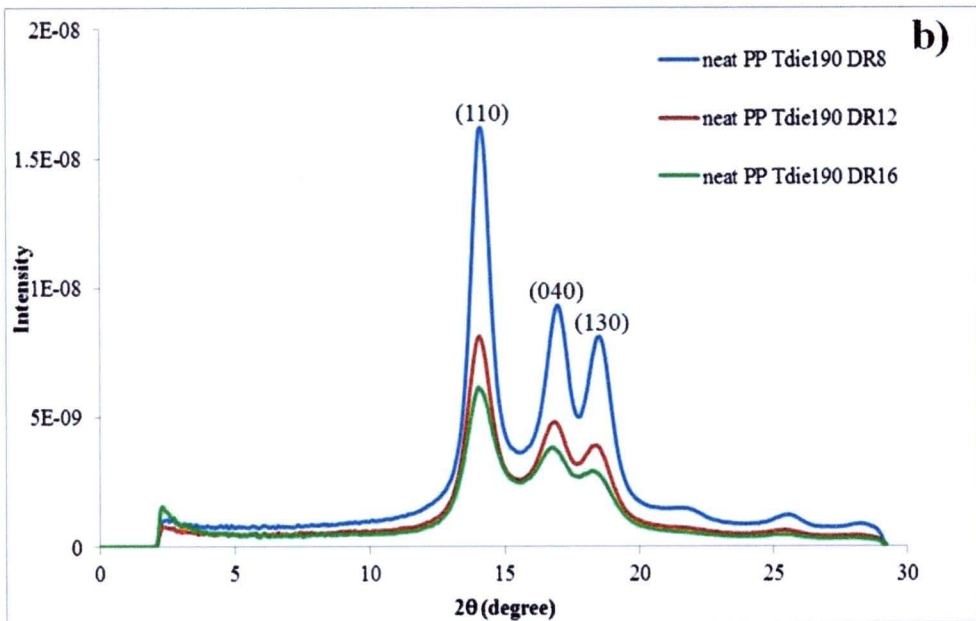
Figure 53 b) Equatorial section of drawn neat iPP fiber at die temperature 190 °C with different draw ratios
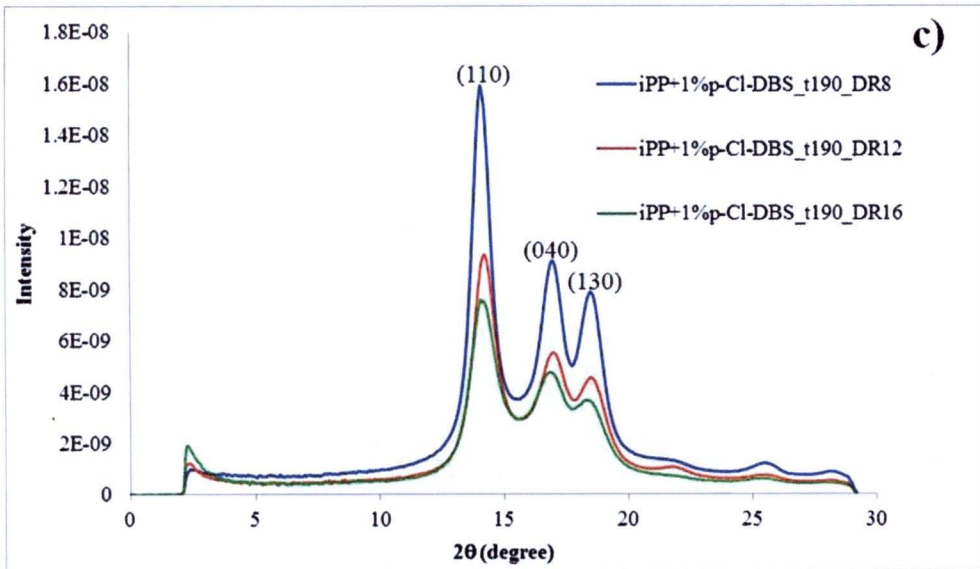
Figure 53 c) Equatorial section of drawn iPP fiber+1%wt of *p*-Cl-DBS d) drawn iPP fiber+1%wt of *p*-Br-DBS at die temperature 190 °C
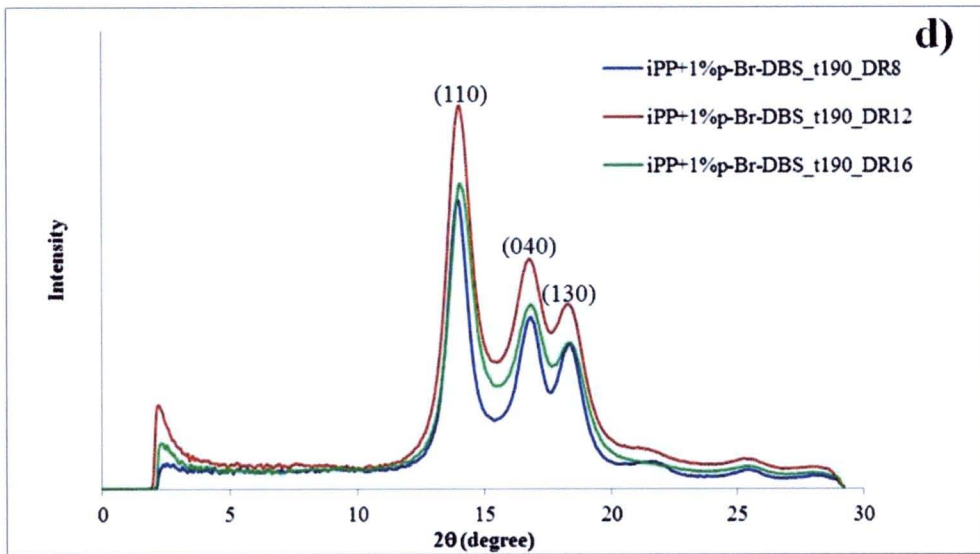
Figure 53 d) Equatorial section of drawn iPP fiber+1%wt of *p*-Br-DBS at die temperature 190 °C

Morphology of as-spun neat iPP fiber and iPP containing sorbitol derivatives

The morphology of as-spun iPP without and with 1 % wt of four different types of sorbitol derivatives after etching with permanganic reagent for 2 hours will be investigated.
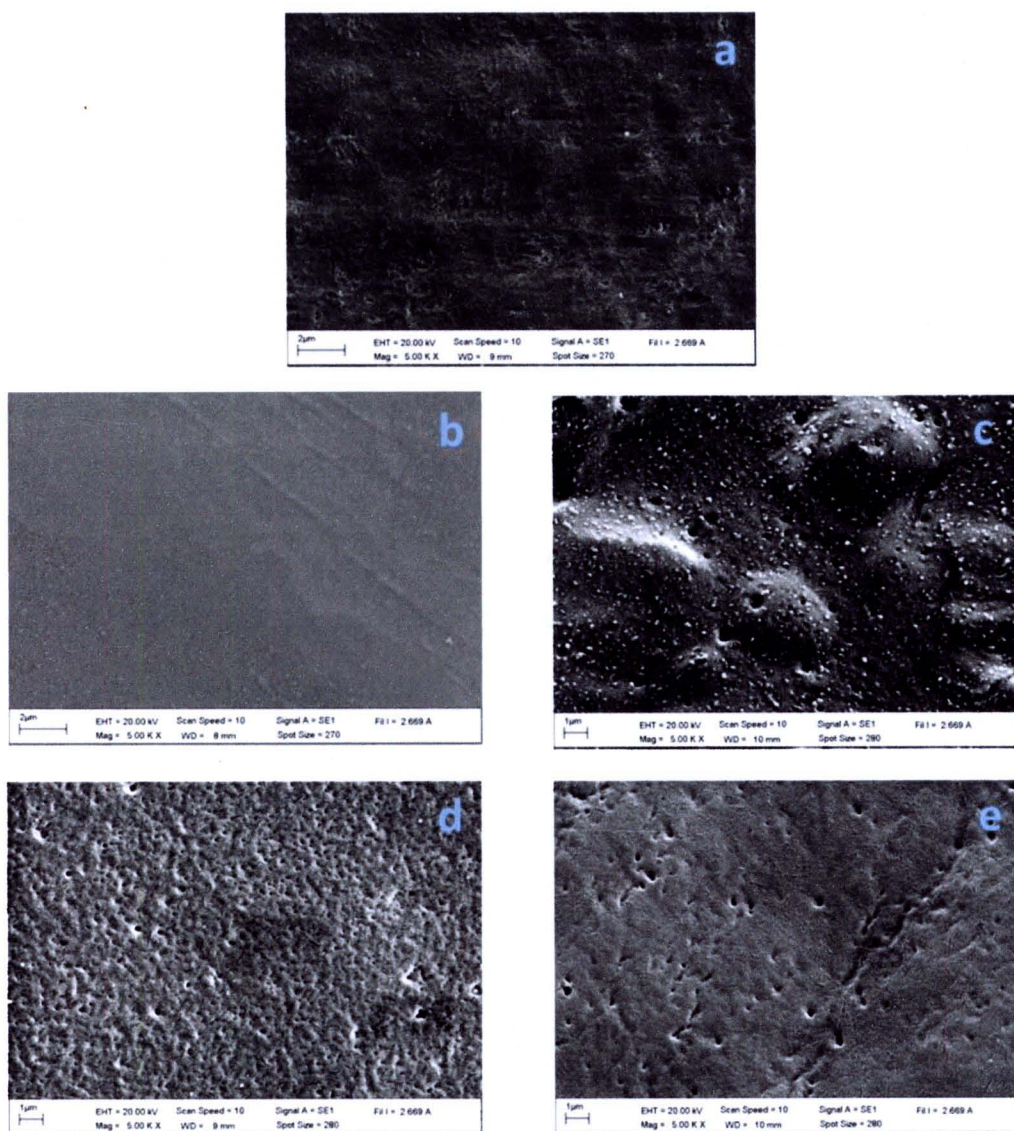
Figure 54 SEM micrographs of cross section morphology of as-spun neat iPP and as-spun iPP with four different types of sorbitol derivatives after etching with permanganic reagent for 2 hours

Figure 54a shows SEM micrograph of etched cross section of neat iPP fiber after etching with permanganic reagent for 2 hours. The micrograph reveals the spherulite of polypropylene which its diameter is about 6.67 μm. Figure 54b shows etched cross section of iPP/1% o-Cl-DBS which is quite smooth surface. Figure 54c, 54d and 54e show SEM micrograph of etched cross section of iPP/1% m-Cl-DBS iPP/1% p-Cl-DBS and iPP/1% p-Br-DBS, respectively. The dark spot can be clearly seen indicating the location of sorbitol derivatives fibrils. Here the fibril has been removed entirely by the etchant and what is displayed is a group of parallel cylindrical hollows. At high magnification, the diameter of the dark are reduce as the observed depth increases. This would arise from the etching mechanism. This process should not give any different features of the hole for indicating the location of sorbitol derivatives fibrils which are perfectly or nearly perfectly aligned.

Table 19 Diameter of sorbitol derivatives fibril and extrude iPP fiber+1% sorbitol derivatives

Sample	Diameter (nm)	Diameter*(nm)
o-Cl-DBS	45.59-216.50	78.76-214.30
m-Cl-DBS	30.08-48.85	107.50-583.33
p-Cl-DBS	50.00-90.00	49.81-219.67
p-Br-DBS	30.00-150.00	83.33-333.33

* extrude iPP fiber+1% sorbitol derivatives

Table 19 shows the diameter of dark spots calculated from Figure 53 are compared with the diameter of fibril in low molecular weight solvent derived from SEM micrographs. It can be seen that the diameters derived from both techniques are similar.

Summary

The high level of preferred orientation of iPP lamellar is clearly seen when the samples were dispersed with small amount of sorbitol derivatives under high screw speed and temperature where the fibril still exist in the polymer melt. The SEM

micrographs of cross section of as-spun iPP fiber were indicated the location of sorbitol derivatives fibrils which aligned within iPP melt.

The effect of sorbitol derivatives on mechanical properties of polypropylene fiber

The mechanical properties of as-spun and drawn fiber were tested by tensile tester (WDW-5E) with full-scale load 100 N and cross head speed 50 mm/min. The specimen gauge length of as-spun and drawn fiber were 20 and 100 mm, respectively.

In this topic, the effect of sorbitol derivatives (i.e. amount, substitution position, and type) and processing condition (i.e. die temperature, screw speed, and draw ratio) on iPP fiber were investigated.

The effect of sorbitol derivatives on mechanical properties of as spun polypropylene fiber

The effect of amount of p-Cl-DBS

Figure 55 deformation behavior curves of as-spun neat iPP and iPP containing different amount of p-Cl-DBS fiber. Diameters of all as-spun fibers were about 0.95 mm. Stress-strain curve indicates of the deformation behavior of material during tensile test.
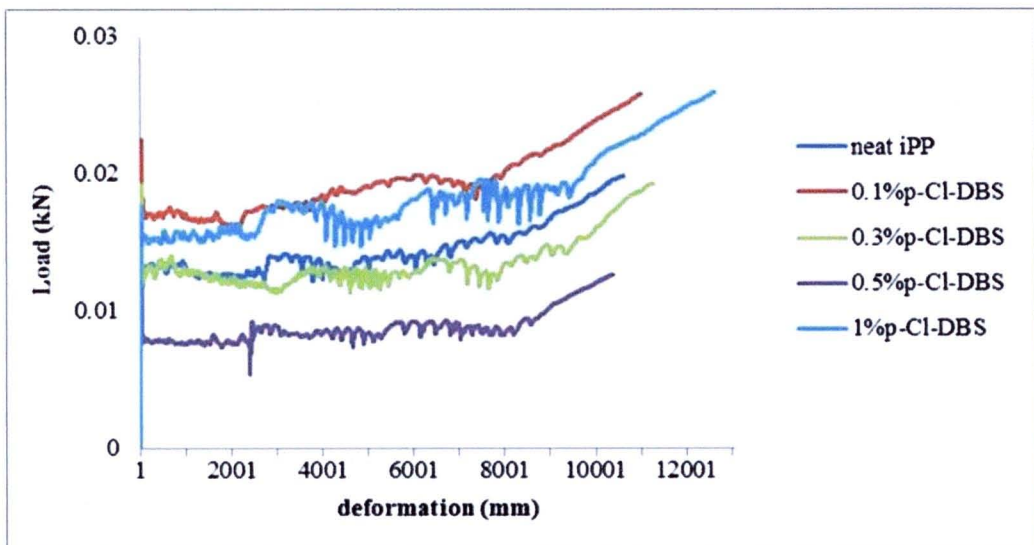
Figure 55 Deformation behaviour curves of as spun neat iPP fiber and as spun iPP containing different concentrations of p-Cl-DBS fiber

The mechanical properties of neat iPP fiber and iPP containing different amounts of p-Cl-DBS fiber were summarized in Table 23. It can be seen that the addition of 1 % wt p-Cl-DBS increase the elastic modulus of iPP fiber up to 48 %.

Table 20 Mechanical properties of as spun neat iPP fiber and as spun iPP containing different concentration of p-Cl-DBS fiber

Sample	Tensile strength at break		Elastic modulus		Percentage of elongation at break	
	MPa		GPa		%	
	Mean	S.D.	Mean	S.D.	Mean	S.D.
Neat iPP	34.70	1.42	0.50	0.11	2645.40	202.73
iPP/0.1%p-Cl-DBS	35.44	3.81	0.48	0.11	2101.61	313.72
iPP/0.3%p-Cl-DBS	26.44	5.70	0.53	0.11	2808.00	591.69
iPP/0.5%p-Cl-DBS	33.63	2.72	0.43	0.08	2847.88	307.40
iPP/1%p-Cl-DBS	29.38	4.07	0.74	0.09	1419.75	804.48
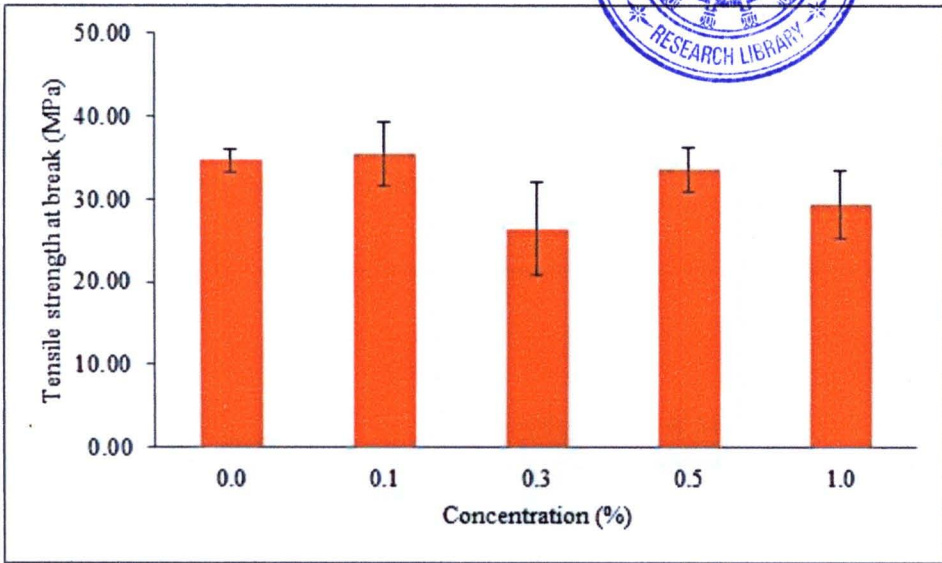
Figure 56 Tensile strength of iPP fiber containing different concentrations of *p*-Cl-DBS
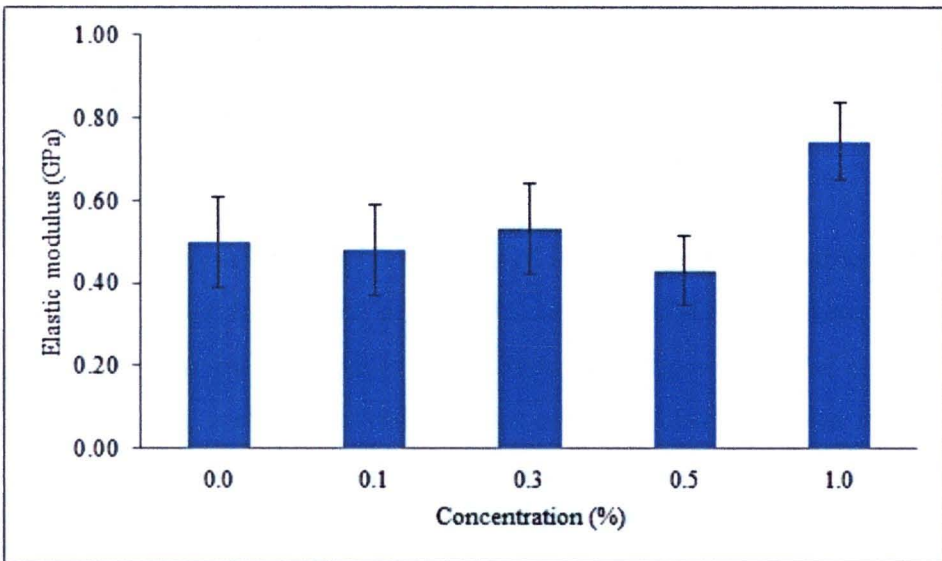
Figure 57 Elastic modulus of iPP fiber containing different concentrations of *p*-Cl-DBS

Figure 56 and Figure 58 show tensile strength and percentage of elongation of neat iPP and iPP containing different amounts of p-Cl-DBS, respectively. It is likely that the amount of p-Cl-DBS has no effect on tensile strength and percentage of elongation of iPP fiber.

Figure 58 Percentage of elongation of iPP fiber containing different concentrations of p-Cl-DBS
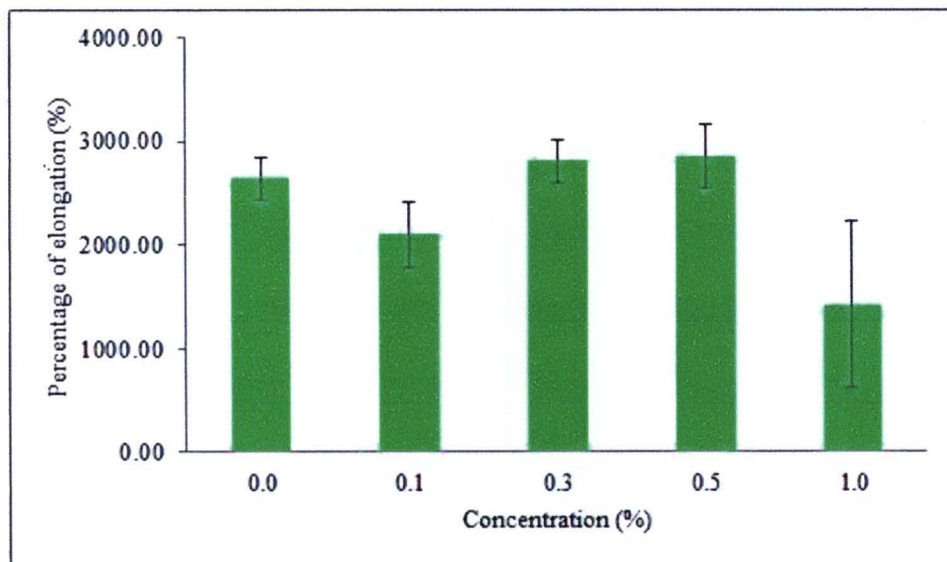
Figure 57 shows the elastic modulus of iPP fiber containing different amount of p-Cl-DBS. It was found that adding 1% wt of p-Cl-DBS increase the elastic modulus of iPP fiber by 46%, while tensile strength and percentage of elongation of iPP fiber containing sorbitol derivatives were not much different from the neat iPP fiber. This is the effect of sorbitol derivatives in nucleation of iPP. High modulus of 1 % wt of p-Cl-DBS in iPP does not come from an increasing in the crystallinity but sorbitol should be involved. Since the crystallinity of iPP and iPP/1% wt of p-Cl-DBS are similar, high modulus of 1% wt of p-Cl-DBS in iPP sample result from the effect of adding sorbitol derivatives on crystallization process of iPP.

The effect of substitution position and type of sorbitol derivatives

Mechanical properties of iPP fiber with the same amount of sorbitol derivatives were displayed in Table 22.

Table 21 Mechanical properties for neat iPP fiber and iPP fiber containing 0.5 % wt of sorbitol derivatives

Sample	Tensile strength at break		Elastic modulus		Percentage of elongation at break	
	MPa		%		GPa	
	Mean	S.D.	Mean	S.D.	Mean	S.D.
Neat iPP	34.70	1.42	0.50	0.11	2645.40	202.73
iPP/0.5%o-Cl-DBS	38.50	3.37	0.59	0.07	2808.60	157.20
iPP/0.5%m-Cl-DBS	31.00	1.31	0.46	0.06	2393.13	537.92
iPP/0.5%p-Cl-DBS	33.63	2.72	0.43	0.08	2847.88	307.40
iPP/0.5%p-Br-DBS	28.13	2.85	0.64	0.08	2339.06	389.57
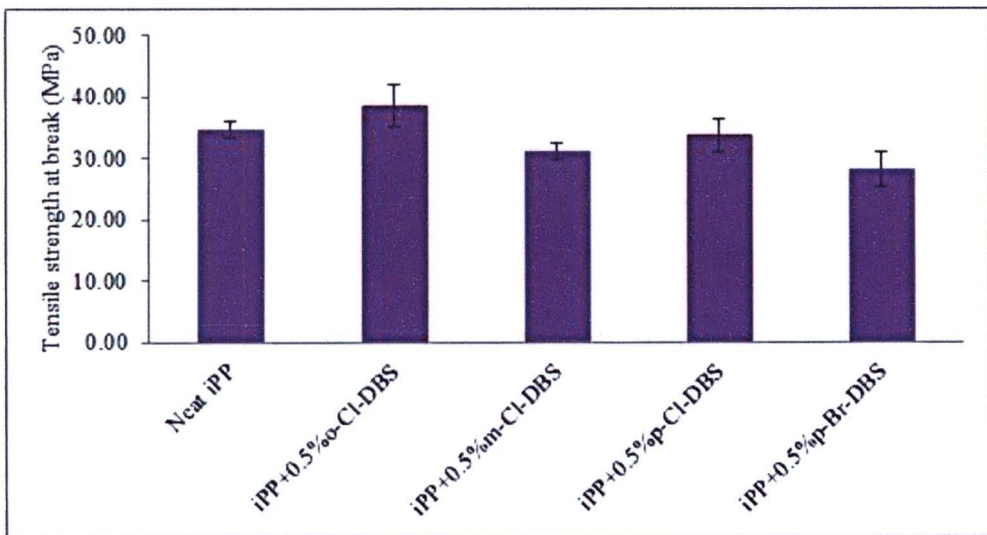
Figure 59 Tensile strength of as spun neat iPP and as spun iPP fiber containing 0.5 % wt of sorbitol derivatives
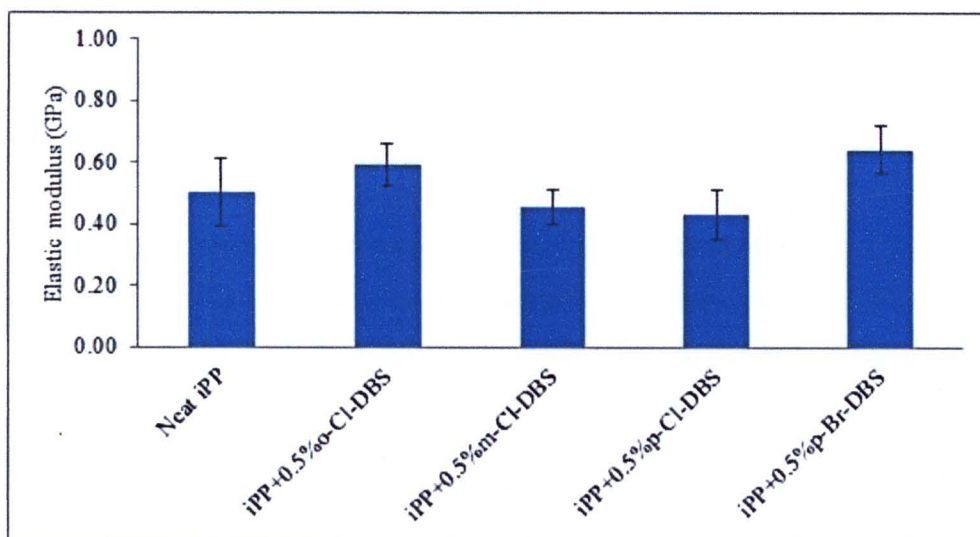
Figure 60 Elastic modulus of as spun neat iPP and as spun iPP fiber containing 0.5 % wt of sorbitol derivatives
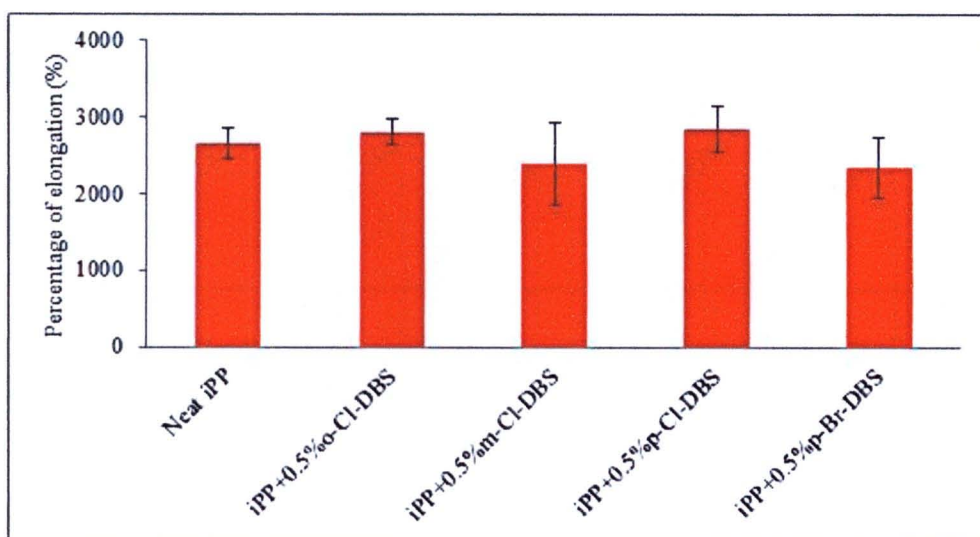
Figure 61 Percentage of elongation of as spun neat iPP and as spun iPP fiber containing 0.5 % wt of sorbitol derivatives

The effect 0.5 % wt of substitution position and type of sorbitol derivatives on mechanical properties of iPP fiber are shown in Table 22. It was found that tensile strength (Figure 59), elastic modulus (Figure 60), and percentage of elongation (Figure

61) of iPP fibers are similar to neat iPP fiber. It is confirmed that the substitution position and type of sorbitol derivatives are not effective on mechanical properties of iPP fiber. This shows similar result as found in the degree of crystallinity of iPP with 0.5 % wt of four different types of sorbitol derivatives.

As the amount of various sorbitol derivatives increased up to 1 % wt, it can be seen that the p-Cl-DBS show an increasing in the elastic modulus (Figure 63) of iPP fiber compared to the other derivatives. While tensile strength and percentage of elongation of iPP-sorbitol derivatives fiber were similar to neat iPP fiber as shown in Figure 62 and Figure 64.

Figure 62 Tensile strength of as spun neat iPP and as spun iPP fiber containing 1
% wt of sorbitol derivatives

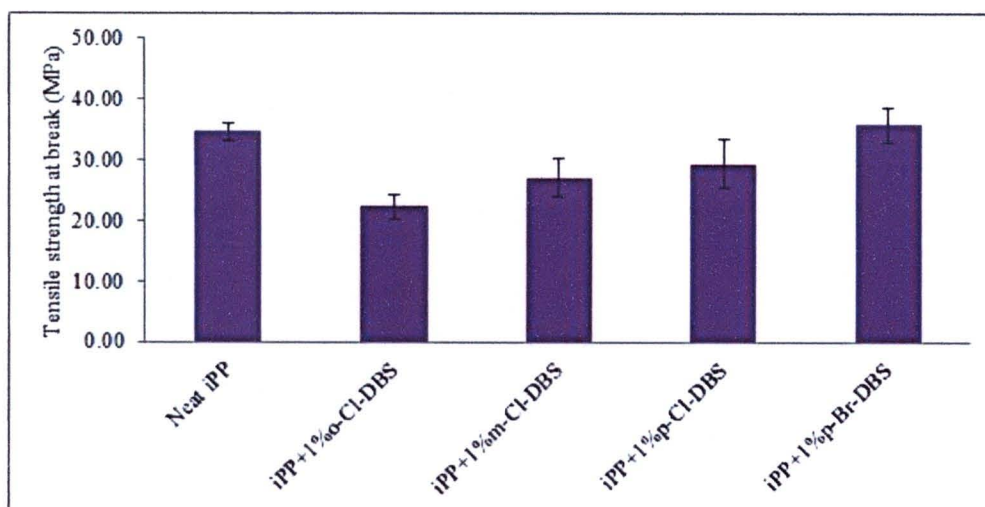**Figure 63 Elastic modulus of as spun neat iPP and as spun iPP fiber containing 1 % wt of sorbitol derivatives**
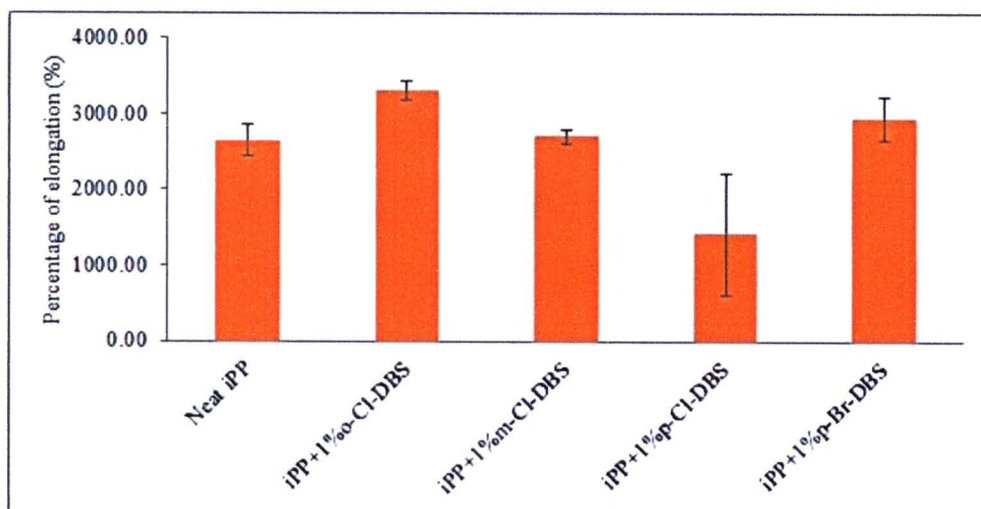
Figure 64 Percentage of elongation of as spun neat iPP and as spun iPP fiber containing 1 % wt of sorbitol derivatives
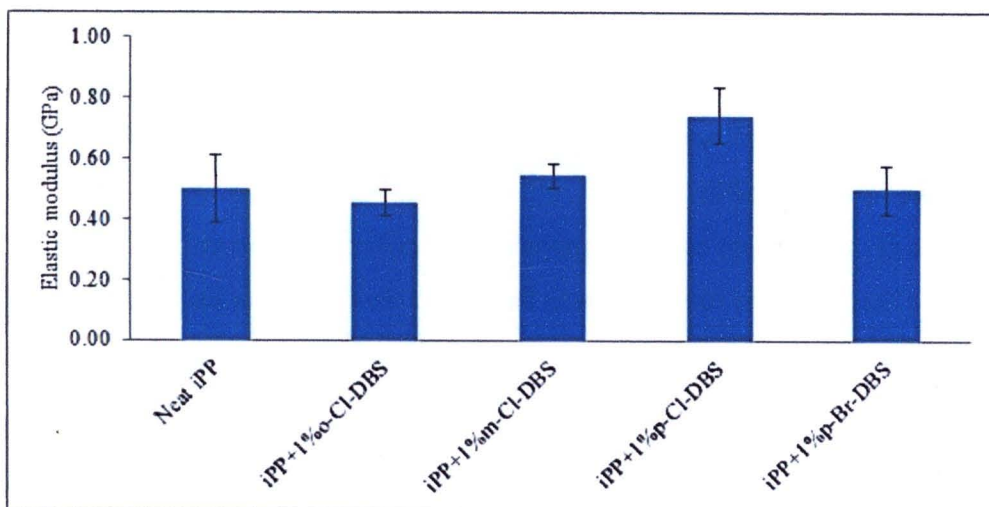
The mechanical properties of as-spun iPP fiber without and with different amount of sorbitol derivatives reveal that the elastic modulus increased up to 48 % when 1 % of *p*-Cl-DBS added. In case of type of sorbitol derivative (*p*-Cl- and *p*-Br-DBS) are not effective on mechanical properties of iPP fiber.

The effect sorbitol derivatives on mechanical properties of drawn polypropylene fiber at different draw ratios

After molten polymer was extruded to form as-spun fiber, it was continuously drawn at 95 °C in glycerol bath. Drawn iPP fibers at different draw ratios from minimum to maximum were collected by varying the take up velocity. In this work, the draw ratios of all samples were calculated from the ratios of the speeds of fast and slow sets of rotating godets.
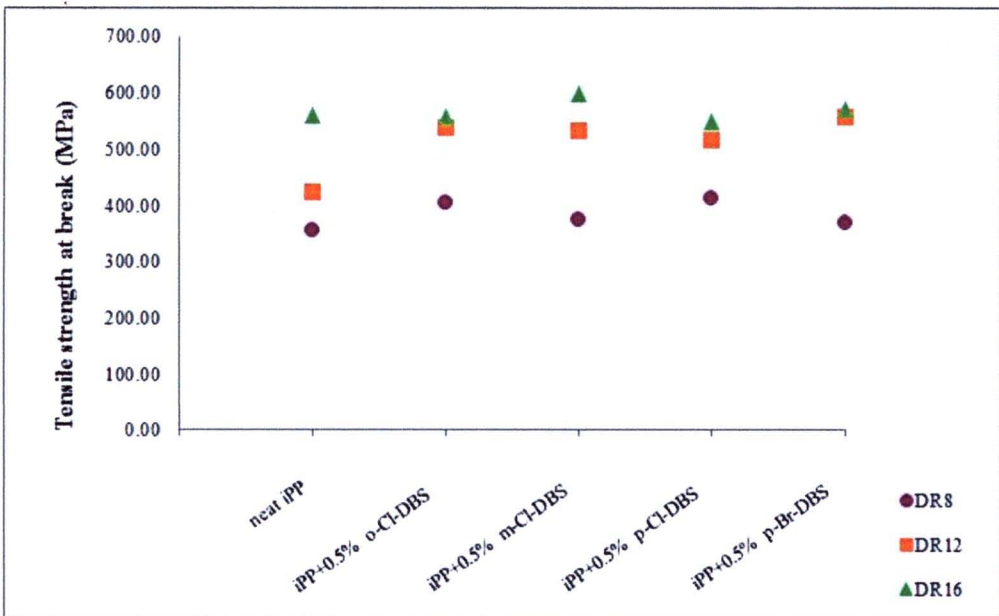
Figure 65 Tensile strength of drawn neat iPP fiber and drawn iPP fiber containing 0.5 % wt of sorbitol derivatives at different draw ratios

The mechanical properties of drawn neat iPP fiber and drawn iPP fiber containing 0.5 % wt of sorbitol derivatives were shown in Figure 65 - Figure 67. Different substitution positions (*ortho*, *meta*, and *para*) for chloro derivatives and type of substituent (Cl and Br) of DBS in iPP fiber sample were investigated in term of die temperature, screw speed, and draw ratio. It was found that the tensile strength and elastic modulus of iPP fiber containing 0.5 % wt of sorbitol derivatives are similar to neat iPP fiber. While percentage of elongation of iPP with 0.5 % wt of sorbitol derivatives decreased when compared to neat iPP.
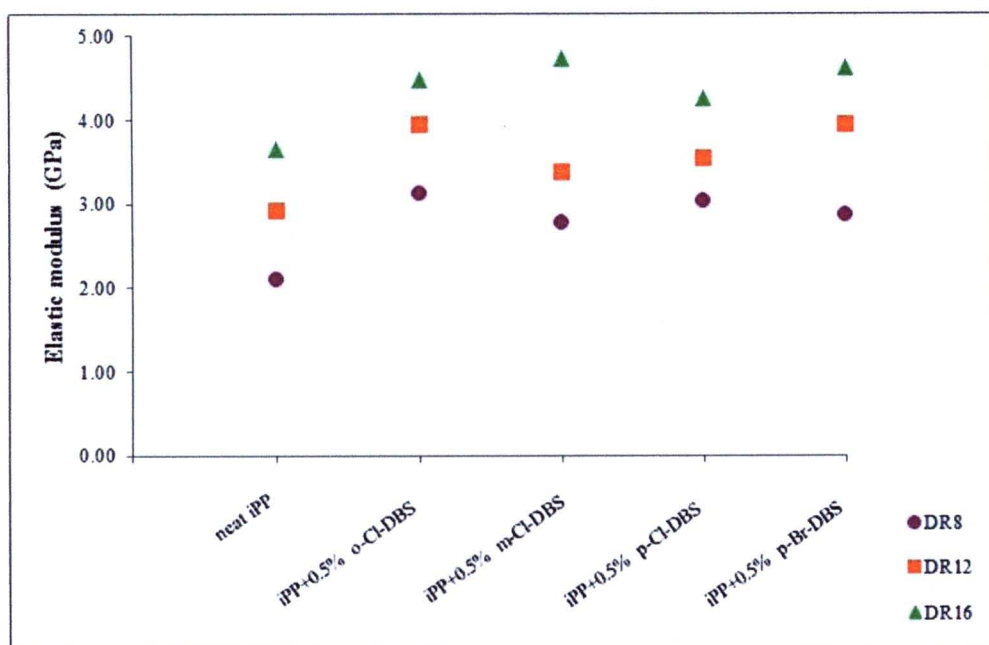
Figure 66 Elastic modulus of drawn neat iPP fiber and drawn iPP fiber containing 0.5 % wt of sorbitol derivatives at diffrent draw ratios

Figure 66 shows elastic modulus of drawn iPP fiber contained 0.5 % wt of sorbitol derivatives, it was found that the elastic modulus of these samples at draw ratio 16 are higher than draw ratio 12 and 8, respectively. The elastic modulus increase linearly with draw ratio increase.

Figure 67 Percentage of elongation of drawn neat iPP fiber and drawn iPP fiber containing 0.5 % wt of sorbitol derivatives at diffrent draw ratios

From the fiber preparation process, the maximum draw ratio that can be drawn is 16. The tensile strength of drawn iPP fiber contained 0.5 % wt of sorbitol derivatives (Figure 67) are similar to drawn iPP fiber at ratio 12. On the other hand it is higher than drawn iPP fiber at ratio 8 about 40 %. This due to at higher draw ratio the iPP crystals giving better orientation along the flow direction than fiber spin at low draw ratio. It is likely the work of Tabatabaei [73] have shown that crystal orientation in cast films is a strong function of the draw ratio (DR). Isotactic polypropylene (iPP) shows increased c-axis orientation with increasing draw ratio, corresponding with improved tensile modulus and yield stress.

As a result, the percentage of elongation of drawn iPP fiber containing 0.5 % wt sorbitol derivatives (Figure 67) decreased with draw ratio increased. This result was obtain from that data of percentage of elongation of drawn iPP fiber contained 0.5 % wt sorbitol derivatives at draw ratio 12 and 8.
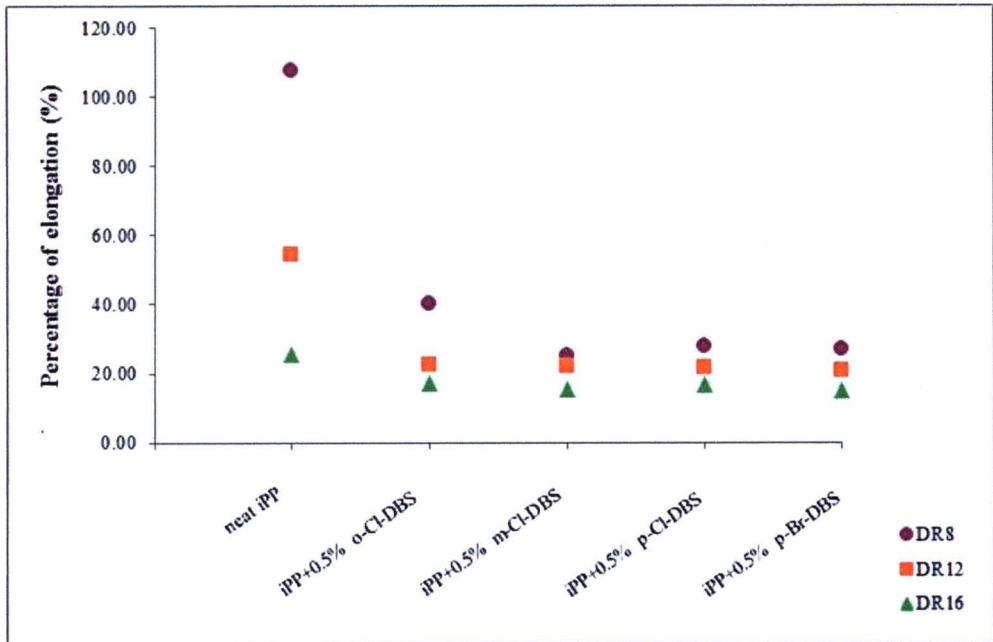
Figure 68 Tensile strength of drawn neat iPP fiber and drawn iPP fiber containing 1 % wt of sorbitol derivatives at diffrent draw ratios

Figure 69 Elastic modulus of drawn neat iPP fiber and drawn iPP fiber containing 1 % wt of sorbitol derivatives at diffrent draw ratios
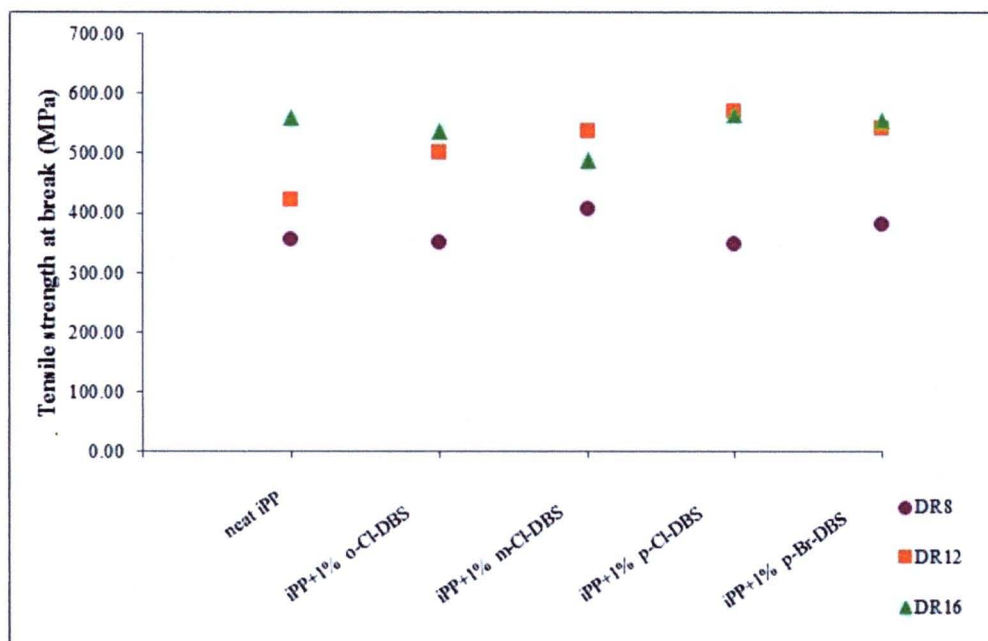

Figure 70 Percentage of elongation of drawn neat iPP fiber and drawn iPP fiber containing 0.5 % wt of sorbitol derivatives at diffrent draw ratios
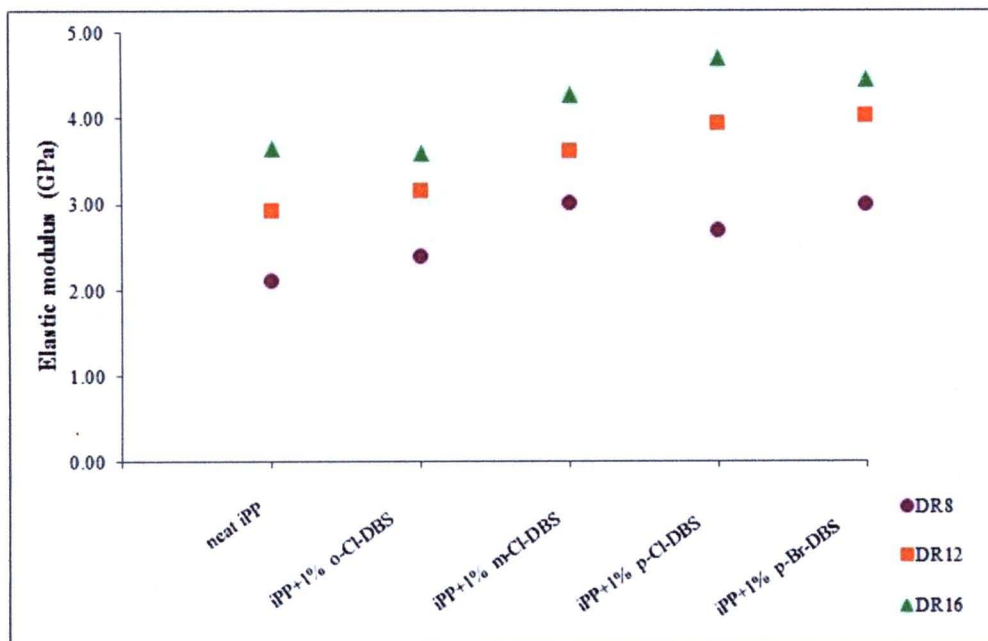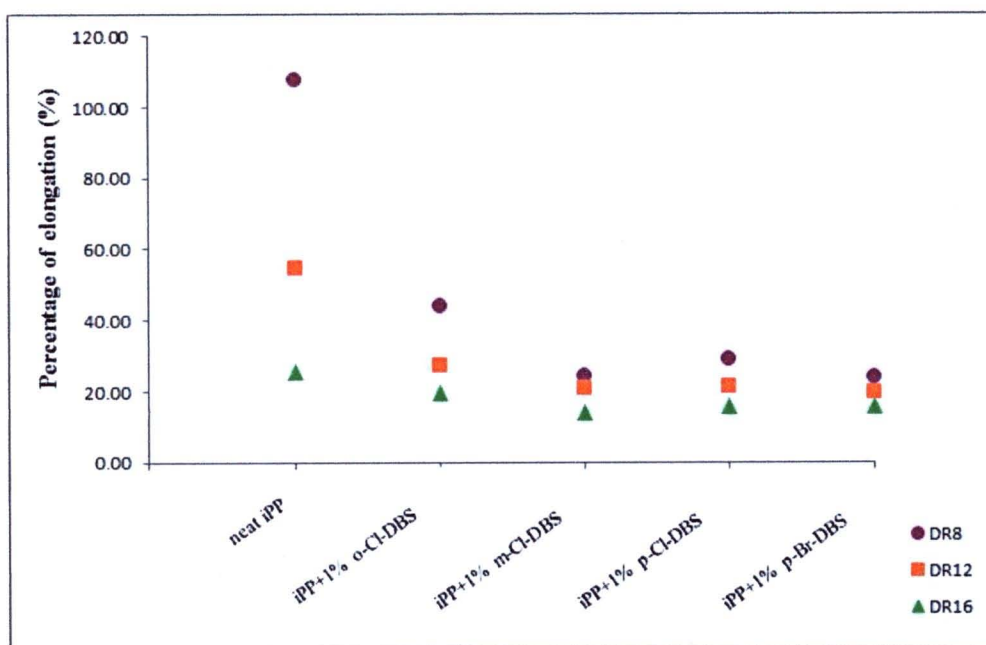
Table 22 Mechanical properties for neat iPP fiber and iPP fiber containing 0.5 % wt of sorbitol derivatives at different draw ratio

Tensile Strength (MPa)										
drawn ratio	Neat iPP		0.5% o-Cl-DBS filled iPP		0.5% m-Cl-DBS filled iPP		0.5% p-Cl-DBS filled iPP		0.5% p-Br-DBS filled iPP	
	Average	S.D.	Average	S.D.	Average	S.D.	Average	S.D.	Average	S.D.
8	356.11	42.11	402.50	30.47	374.38	29.45	411.11	32.57	368.13	36.93
12	422.22	24.12	638.13	45.43	531.88	47.35	516.67	23.05	556.25	28.75
16	560.00	40.88	536.88	37.51	596.88	24.63	549.00	21.32	549.38	29.81

Elastic Modulus (GPa)										
drawn ratio	Neat iPP		0.5% o-Cl-DBS filled iPP		0.5% m-Cl-DBS filled iPP		0.5% p-Cl-DBS filled iPP		0.5% p-Br-DBS filled iPP	
	Average	S.D.	Average	S.D.	Average	S.D.	Average	S.D.	Average	S.D.
8	2.09	0.48	3.13	0.27	2.77	0.27	3.04	0.28	2.86	0.30
12	2.92	0.25	3.94	0.48	3.38	0.13	3.54	0.35	3.95	0.17
16	3.65	0.14	4.47	0.53	4.73	0.37	4.25	0.42	4.62	0.36

Percentage of Elongation at break (%)										
drawn ratio	Neat iPP		0.5% o-Cl-DBS filled iPP		0.5% m-Cl-DBS filled iPP		0.5% p-Cl-DBS filled iPP		0.5% p-Br-DBS filled iPP	
	Average	S.D.	Average	S.D.	Average	S.D.	Average	S.D.	Average	S.D.
8	107.67	28.95	40.13	7.02	25.19	3.34	27.67	1.84	26.94	7.97
12	54.44	13.50	22.25	1.93	22.00	3.36	21.61	3.84	20.63	2.89
16	25.44	2.19	17.19	4.83	15.19	0.96	16.60	2.47	14.88	1.46

At 1 % wt of sorbitol derivatives, it was found that the tensile strength, elastic modulus, and percentage of elongation (Table 24) are similar to the results at 0.5 % wt of sorbitol derivatives for the same condition (Table 23). This indicates that the mechanical properties are controlled by the draw process not additive in this case. When drawn iPP fiber, force are sufficient for chain tilt and slip within the lamellae. The lamellae are deformation by chain slip that a creak develops. The partial unfolded chains that link the creak lead to successive tearing off of crystal blocks from the lamellae into microfibrils. For polyolefin fiber all repeating unit of molecular chains

consist of only carbon and hydrogen atoms. Thus, the densities of crystalline and amorphous orientation are not much different [9].

Table 23 Mechanical properties for neat iPP fiber and iPP fiber containing 1 % wt of sorbitol derivatives at different draw ratio

	Tensile Strength at break (MPa)									
drawn ratio	Neat iPP		1% o-Cl-DBS filled iPP		1% m-Cl-DBS filled iPP		1% p-Cl-DBS filled iPP		1% p-Br-DBS filled iPP	
	Average	S.D.	Average	S.D.	Average	S.D.	Average	S.D.	Average	S.D.
8	356.11	42.11	349.38	6.78	406.88	28.65	347.50	41.75	381.88	29.27
12	422.22	24.12	500.63	42.21	536.25	37.11	571.25	29.25	541.88	27.64
16	560.00	40.88	536.25	35.53	488.75	32.60	566.25	26.02	555.63	24.41

	Elastic Modulus (GPa)									
drawn ratio	Neat iPP		1% o-Cl-DBS filled iPP		1% m-Cl-DBS filled iPP		1% p-Cl-DBS filled iPP		1% p-Br-DBS filled iPP	
	Average	S.D.	Average	S.D.	Average	S.D.	Average	S.D.	Average	S.D.
8	2.09	0.48	2.38	0.05	3.01	0.29	2.69	0.32	2.99	0.34
12	2.92	0.25	3.15	0.21	3.62	0.19	3.94	0.09	4.03	0.10
16	3.65	0.14	3.60	0.23	4.28	0.21	4.70	0.14	4.45	0.32

	Percentage of Elongation at break (%)									
drawn ratio	Neat iPP		1% o-Cl-DBS filled iPP		1% m-Cl-DBS filled iPP		1% p-Cl-DBS filled iPP		1% p-Br-DBS filled iPP	
	Average	S.D.	Average	S.D.	Average	S.D.	Average	S.D.	Average	S.D.
8	107.67	28.95	43.81	17.23	24.19	3.84	28.88	5.50	23.75	3.67
12	54.44	13.50	27.38	2.13	20.69	1.87	21.13	1.69	19.63	2.56
16	25.44	2.19	19.31	2.17	13.81	1.00	15.44	0.32	15.50	1.16

In case of drawn fiber, amount and types of sobitol derivatives show no effect on mechanical properties of iPP. On the other hand, at draw ratio 16, the fiber shows higher tensile strength and elastic modulus. This is due to high orientation of iPP crystals along the fiber direction. These orientations generally increase with increasing draw ratio fiber, resulting in the increases in modulus and tensile strength [9]. This is similar to the study of Lipp [8] and Fujiyama [74]. They also reported that, the orientation results in highly anisotropic mechanical properties, with significantly higher tensile modulus and yield stress in the flow direction.

Summary

The effect of sorbitol derivatives on mechanical properties of as-spun and drawn iPP fiber were studied by using tensile tester. For as-spun fiber, the effect of amount, substitution position, and type of sorbitol derivatives on mechanical properties of iPP fiber reveals that the elastic modulus of neat iPP can be increased up to 48 % when 1% wt of *p*-Cl-DBS added. For drawn iPP fiber, the tensile strength and elastic modulus of both amount of sorbitol derivatives (0.5 and 1 % wt) fiber increase when draw ratio increased. While the percentage of elongation of fiber decrease when draw ratio increased. The sorbitol derivatives have no effect on mechanical properties for drawn fiber.